Technical report: validation of model datasets used in Early-warning system:

Climate-smart spatial management of UK fisheries, aquaculture and conservation

Authors: Susan Kay, Sevrine Sailley, John Aldridge, Robert McEwan, Elizabeth Talbot, Robert Wilson

Contents

1 Overview

This report provides validation information for the model projections used in the MSPACE meta-analysis. **The focus of the validation is on the ability of models to represent spatial variability and temporal trends on a decadal time scale.** The MSPACE meta-analysis compares present state against future state by looking at the change in the mean value of each variable at each model grid cell, weighted by standard deviation. This means that it is more important for the model to capture changes over time and the variation from place to place than to match absolute values of the observations, and we have therefore not included dataset bias in our assessments.

Several models were used to produce the datasets. The validation does not aim to assess the skill of the models per se, but to provide an expert judgement on how confident we are in the use of the model outputs as applied in MSPACE. This report provides information about the model, the evidence base used to assess the model outputs against observed values, and a summary of whether we have strong, moderate or weak confidence in the use of different model-derived variables in different parts of UK seas. In some cases there was insufficient observational evidence to make an assessment, but we have been able to assign a confidence level for most variables. The evidence presented here will enable expert users to make a judgement as to whether our assessment is appropriate for a particular application of the MSPACE outputs.

The ultimate driver for all the model outputs used in MSPACE is global climate modelling. This aims to simulate large-scale patterns in climate-driven variables, but does not attempt to precisely match real-world conditions in any given year in either hindcast or future projections. We therefore only consider trends over a period of a decade or longer.

Except for in the fish species modelling, section 5, only one regional climate model has been used, so we were unable to assess inter-model uncertainty and this is not included in the confidence levels presented here. The global climate model on which the regional modelling was based, MPI-ESM-LR, gives projections for future change in European seas which are low to moderate compared to comparable climate models (i.e. the CMIP5 set, which contributed to the 5th Assessment Report of the Intergovernmental Panel on Climate Change). The projections should be considered as representative of possible future change, with the two climate scenarios RCP4.5 and RCP8.5 giving an indication of range, but more extreme change is also possible.

The tables in section 2 summarise our confidence assessment for each of the variables used as inputs to the early warning system. The basis for this assessment is given in sections 3-7, separated according to the model that provided the dataset: water column environmental variables produced by the POLCOMS-ERSEM pelagic model are in section 3, seabed variables produced by the ERSEM benthic model in section 4, fish species abundance produced by the SS-DBEM model in section 5, crab (*Cancer pagurus*) distribution produced by a dedicated DEB model in section 6 and seaweed (*S. latissima*) production from another DEB model in section 7. Model names are given in full in their respective sections, along with a brief description of the model and the methods used to validate the dataset. The type of analysis and presentation is different for each section, according to the amount and nature of observational evidence available.

2 Summary of confidence assessment

confidence
strong
moderate
weak
data deficient

Conservation

	UK EEZ	England	Wales	Scotland	N. Ireland
Surface dissolved oxygen					
Surface sea water pH					
Surface sea water potential temperature					
Surface sea water salinity					
Surface thermal fronts					
Heatwave duration					
Water column sum of phytoplankton carbon					
Net primary production					
Potential Energy Anomaly (stratification)					
Water column sum of phytoplankton carbon					
Bottom dissolved oxygen					
Bottom non-living organic carbon					
Bottom saturation state of aragonite					
Bottom sea water pH*					
Bottom sea water potential temperature					
Bottom sea water salinity					
Atlantic cod - *Gadus morhua*					
Haddock - *Melanogrammus aeglefinus*					
European hake - *Merluccius merluccius*					
Common squid - *Loligo forbesii*					
Common sole - *Solea solea*					
Saithe - *Pollachius virens*					
Whiting - *Merlangius merlangus*					
Blue mussel - *Mytilus edulis*					
Sediment carbon (available and refractory)					
Depth of the oxygen horizon					
Brown crab - *Cancer pagarus*					
Common shrimp - *Crangon crangon*					
European plaice - *Pleuronectes platessus*					

Fisheries

	UK EEZ	England	Wales	Scotland	N. Ireland
Atlantic herring - *Clupea harengus*					
European bass - *Dicentrarchus labrax*					
Common squid - *Loligo forbesii*					

Whiting - *Merlangius merlangus*					
Blue whiting - *Micromesistius poutassou*					
European pilchard - *Sardina pilchardus*					
Atlantic mackerel - *Scomber scombrus*					
European sprat - *Sprattus sprattus*					
Horse mackerel - *Trachurus trachurus*					
Common shrimp - *Crangon crangon*					
Atlantic cod - *Gadus morhua*					
Atlantic halibut - *Hipoglossus hipoglossus*					
Common monkfish - *Lophius piscatorius*					
Haddock - *Melanogrammus aeglefinus*					
European hake - *Merluccius merluccius*					
Blue mussel - *Mytilus edulis*					
Nephrops - *Nephrops norvegicus*					
European plaice - *Pleuronectes platessus*					
Pollock - *Pollachius pollachius*					
Saithe - *Pollachius virens*					
Turbot - *Scophthalmus maximus*					
Common sole - *Solea solea*					
Brown crab - *Cancer pagurus*					

Aquaculture

	UK EEZ	England	Wales	Scotland	N. Ireland
Seaweed (sugar kelp - *Saccharina latissima*)					
Atlantic salmon - *Salmo salar*					
Blue mussel - *Mytilus edulis*					
Surface sea water potential temperature					
Heatwave duration					
Surface dissolved oxygen					
Surface sea water pH					
Surface saturation state of aragonite					
Net primary production					
Potential Energy Anomaly (stratification)					
Water column sum of phytoplankton carbon					
Bottom dissolved oxygen					
Bottom non-living organic carbon					
Bottom saturation state of aragonite					
Bottom sea water pH*					
Bottom sea water potential temperature					
Bottom sea water salinity					

3 Environmental variables in the water column (POLCOMS-ERSEM pelagic)

This section gives validation information about the physical and biogeochemical water column variables used in the conservation meta-analysis:

- surface and bottom level dissolved oxygen, temperature, salinity, pH and aragonite saturation state
- column total primary production
- potential energy anomaly
- location of thermal fronts
- column total phytoplankton biomass
- bottom level organic carbon

These variables come from the coupled model POLCOMS-ERSEM (described below), used in a climate model configuration.

3.1 Model description: the POLCOMS and ERSEM models

ERSEM, the European Regional Seas Ecosystem Model (Blackford et al., 2004; Butenschön et al., 2016), simulates marine biogeochemical cycling and the lower trophic levels of the marine ecosystem. It is one of the more complex models of its type and is well suited to modelling coastal and shelf sea environments; it has a long track record of use for the North West European Shelf. To produce the dataset used here it was coupled to the physical model POLCOMS, the Proudman Oceanographic Laboratory Coastal Ocean Modelling System (Holt and James, 2001), which tracks the transfer of matter and energy through the system. The climate change signal was applied by using outputs from climate models at the atmosphere-ocean surface, at the open ocean boundary and for river inputs (see section 3.1.1).

ERSEM (Figure 3.1) tracks the cycling of carbon, nitrogen, phosphorus and silicate in the marine environment. Primary producers are modelled as four functional types of phytoplankton: diatoms, which use silicate, and the size-based classes pico-, nano- and micro- phytoplankton. Zooplankton are represented as three size-based functional types: heterotrophic nanoflagellates, microzooplankton and mesozooplankton. Particulate organic matter is separated into three size classes and dissolved organic matter is split in to labile, semi-labile and refractory components. There is also a bacterial loop, with one bacterial type. Carbon and nutrients move between all these components through processes such as photosynthesis, nutrient uptake and predation; there is fully flexible stoichiometry, with no fixed ratios imposed. The carbon to chlorophyll ratio for each functional type can also vary depending on the levels of light and available nutrients. A separate benthic model handles transfers at the sea bed and within sediment, see section 4 for more information. The carbonate system is also included in the model, enabling it to produce outputs such as pH and the saturation state of aragonite.

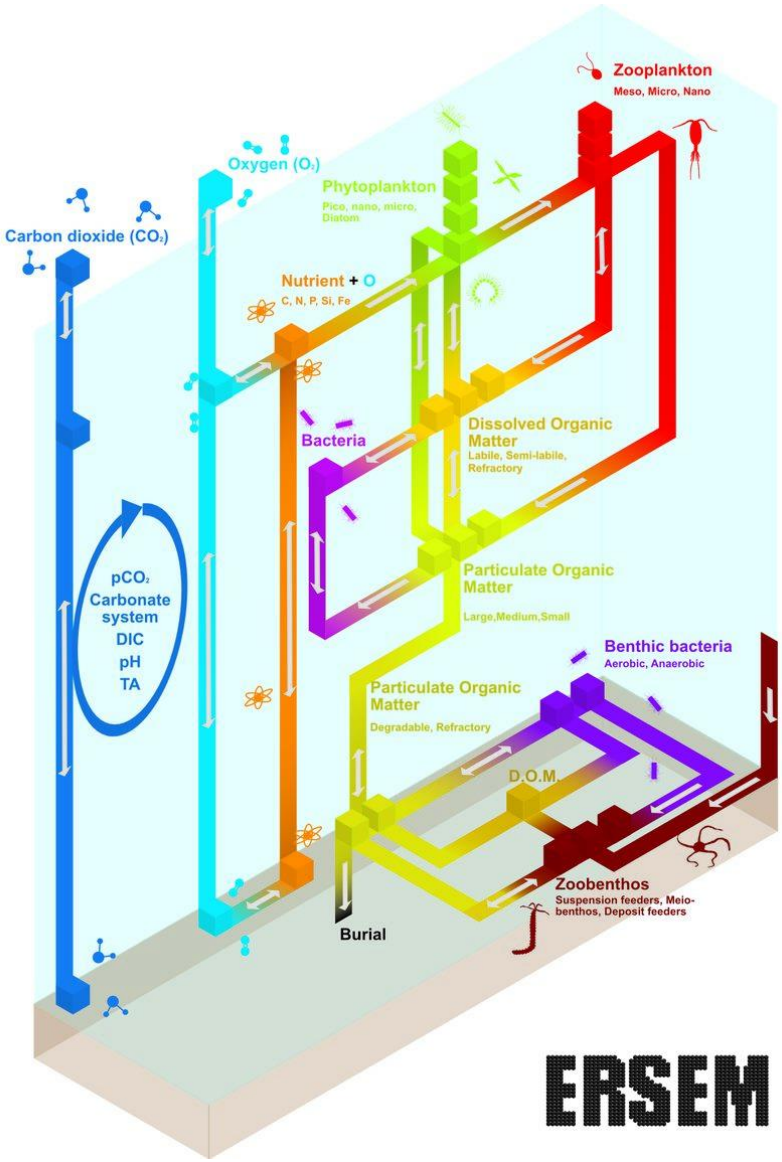

Figure 3.1 Schematic of ERSEM, the European Regional Seas Ecosystem Model. Each cube represents separate parts of the ecosystem. For example, phytoplankton is represented by four separate functional types. Fluxes within the ecosystem are represented by arrows.

The physical environment was simulated by POLCOMS, a regional circulation model which is able to model the varying depths and steep bathymetry of the waters around the UK and has been applied to coastal waters globally (Barange et al., 2014; Holt et al., 2009). It uses surface conditions of winds, temperature, pressure, and radiation to model water circulation and transfers of energy and momentum laterally and vertically through the water column. POLCOMS is a free surface model with time-varying depth, and it includes tides but not waves. The model was run on a domain extending over the northwest European shelf and the Mediterranean Sea (Figure 3.2), but only waters around the British Isles have been included in the analysis presented here. The resolution was 0.1° for both latitude and longitude (6-11 km); vertically the model used a modified-sigma scheme, with 40 vertical points at each grid cell regardless of depth, enabling good representation of both deep and shallow waters. The temperature and salinity outputs from POLCOMS were used directly in MSPACE and they also provided the environmental conditions for ERSEM, which ran within each grid cell of POLCOMS at every time step.

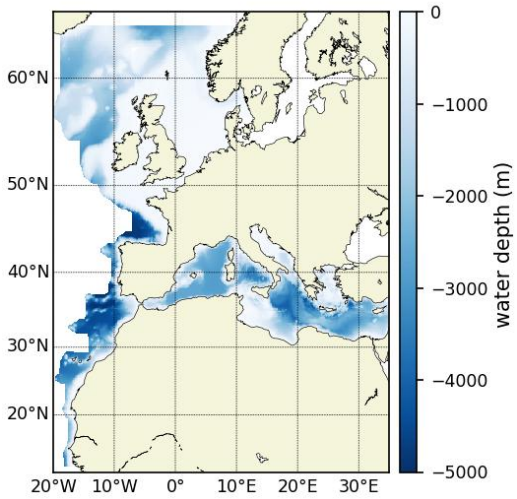

Figure 3.2: The POLCOMS-ERSEM model domain, showing water depth.

Model outputs for 2006 to 2099 and further documentation can be found in the Copernicus Climate Data Store (DOI: 10.24381/cds.dcc9295c).

3.1.1 Implementation: scenarios, spatial and temporal scale.

The POLCOMS-ERSEM coupled model was used to create projections for the 21st century for two greenhouse gas concentration scenarios, using the standard IPCC Representative Concentration Scenarios (RCPs) (Meinshausen et al., 2011). The moderate RCP4.5 scenario has concentrations rising until mid-century then stabilising, under the more extreme RCP8.5 scenario they continue to rise throughout the century. The scenarios start in 2006, and for years before that there is a "historical" period which uses observed values of atmospheric CO_2. Differences between the two scenarios emerge from the 2030s onwards. Climate change was applied to the model by using surface and ocean boundary conditions from a global climate model taken from the Coupled Model Intercomparison Project Phase 5 (CMIP5; (Taylor et al., 2011)). The global model used was the Max Planck Institute-Earth System Model-Low Resolution (MPI-ESM-LR); its projections for future conditions in Europe are generally in the low to moderate part of the CMIP5 range.

Forcing data for the atmospheric surface used MPI-ESM-LR downscaled to a resolution of 0.11° using the Rossby Centre Regional Atmospheric Model (RCA4) and taken from the EURO-CORDEX set (www.cordex.org). Physical and biogeochemical ocean boundary conditions were taken from the global MPI-ESM-LR model.

River inputs of freshwater, nitrate and phosphate were taken from the hydrological model E-HYPE (Donnelly et al., 2016), which was run using inputs from the same global model and a business-as-usual nutrient scenario. Climatological water and nutrient flows were used at the Baltic boundary, and these were kept constant through the modelled period.

The model was run continuously for 1970-2099, with separate climate scenarios RCP4.5 and RCP8.5 for 2006 onwards. All model outputs used in the MSPACE analysis were monthly means. Temperature and salinity were taken directly from POLCOMS; potential energy anomaly and the

location of thermal fronts were calculated from daily values of these outputs. Dissolved oxygen, pH, primary production, phytoplankton biomass, organic carbon and aragonite saturation state were taken from the ERSEM pelagic model.

The POLCOMS-ERSEM outputs of temperature, salinity, oxygen, pH and primary production were used as inputs for one set of the SS-DBEM runs used in the fish modelling (section 5) and for the carb and seaweed modelling (sections 6 and 7).

3.2 Validation methodology

3.2.1 Validation datasets

Validation was based on comparison to publicly available observational datasets, supplemented by data from project partners, where needed, to fill gaps. The data sources are listed here and summarised in Table 3.1.

Temperature, salinity and oxygen observations were taken from the North Sea Biogeochemical Climatology version 1.1 (NSBC, Hinrichs et al., 2017). This is based on data from multiple sources including ICES, EMODnet and the World Ocean Database, for years to 2014, and covers an extended North Sea region, 47°N to 65°N, 15°W to 15°E. Additional observations for temperature and salinity were taken from the Hydrographic Climatology of the North Sea and Surrounding Regions version 2.0 (KNSC, Bersch et al., 2016). This covers the same region as the NSBC and is based on the same datasets, however it includes all available temperature and salinity measurements whereas NSBC only includes those collected in association with biogeochemical data. Climatological gridded mean values (NSBC level 3) were used for comparison of spatial patterns, monthly box-averages of quality controlled data (level 2) were used for temporal trends.

Sea surface temperature (SST) was also compared to satellite observations, using the ESA SST CCI and C3S product prepared for the European Space Agency Climate Change Initiative and the Copernicus Climate Change Service, and sourced from the Copernicus Marine Service, https://doi.org/10.48670/moi-00169.

Spatial patterns of surface and bottom level pH and bottom level aragonite saturation were taken from the Global Ocean Data Analysis Project version 2 (GLODAPv2) mapped product (Lauvset et al., 2016).

Primary production was assessed by comparing to previously published values for the North Sea (Capuzzo et al., 2018) and to satellite estimates from the Copernicus Globcolour global product (https://doi.org/10.48670/moi-00281).

Systematic observations of phytoplankton biomass and bottom level organic carbon were not available. Surface chlorophyll derived from ocean colour satellite observations was used to give an indication of spatial and temporal variability in phytoplankton biomass. The data set used was the European Space Agency Climate Change Initiative (ESA-CCI) multi-sensor global ocean colour product, sourced from the Copernicus Marine Service, https://doi.org/10.48670/moi-00283.

Table 3.1 Summary of validation data sources. Abbreviations are explained in the text above.

Variable	Spatial variation	Temporal variation	Years available
Dissolved oxygen	NSBC level 3	NSBC level 2	1980-2014
Temperature	NSBC level 3, satellite SST	KNSC, satellite SST	1980-2014 1982-2021

Salinity	NSBC level 3	KNSC	1980-2014
pH	GLODAP gridded climatology	see section 3.3.7	1980-2014
Aragonite saturation state	GLODAP gridded climatology	n/a	1980-2014
Primary production	Globcolour satellite; Capuzzo et al., 2018	Globcolour satellite; Capuzzo et al., 2018	1998-2022 1988-2013
Potential energy anomaly	From T and S assessment	From T and S assessment	
Location of thermal fronts	From SST assessment	From SST assessment	
Phytoplankton biomass	CCI satellite	CCI satellite	1998-2021
Bottom level organic carbon	n/a	n/a	

3.2.2 Methods used to compare model outputs to observations

Model-observation comparison was based on UK national areas and the whole UK Exclusive Economic Zone (EEZ) (Figure 3.3). Where sufficient observational evidence was available the national areas were separated into inshore and offshore sections.

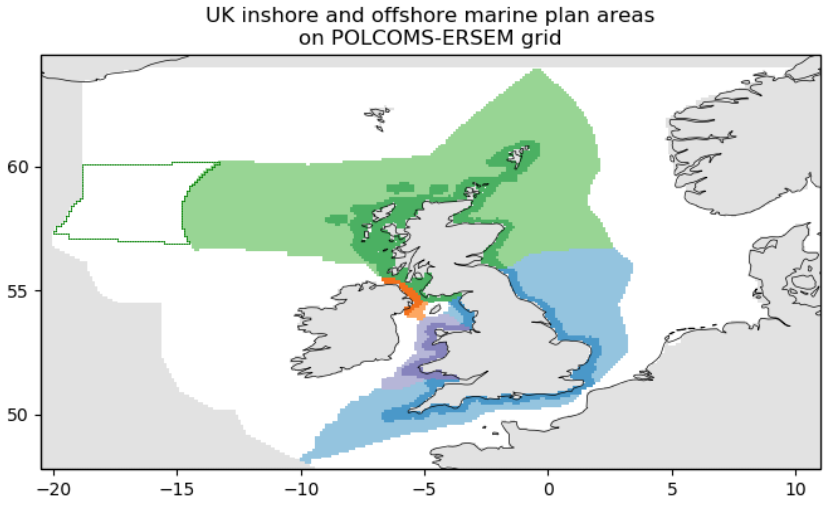

Figure 3.3. National areas within the UK EEZ on the POLCOMS-ERSEM model grid. Inshore areas, as defined in national marine plans, are shown in a darker shade. The Hatton area of Scotland, outlined in green, is outside the UK EEZ and has not been included in this analysis.

The overall aim of the validation was to evaluate how well the model-derived dataset represented spatial variation and temporal trends in the variables used for MSPACE. Where available, a gridded climatology of annual mean values based on observations was used to investigate how well the model captures observed spatial variation. A model climatology was calculated, matching the time-period of the observational climatology as closely as possible, and maps of the two climatologies are presented side-by side for qualitative comparison. For quantitative analysis, the model and observational climatologies were interpolated to the same grid, using nearest-neighbour

interpolation to the coarser of the two grids. Then, for each region, the standard deviation for the model and observational datasets and the Pearson correlation coefficient between them were calculated using all grid points in that region, as follows:

$$standard\ deviation = \sqrt{\frac{1}{N}\sum_{i=1}^{N}(x_i - \bar{x})^2}$$

$$correlation\ coefficient = \frac{\sum_{i=1}^{N}\left(x_i^{model} - \overline{x^{model}}\right)\left(x_i^{obs} - \overline{x^{obs}}\right)}{\sqrt{\sum_{i=1}^{N}(x_i^{model} - \overline{x^{model}})^2 \sum_{i=1}^{N}(x_i^{obs} - \overline{x^{obs}})^2\left(x_i^{obs} - \overline{x^{obs}}\right)^2}}$$

$\overline{x_i^{model}}$, $\overline{x_i^{obs}}$ is the climatological mean value of the model or observation at the i^{th} grid point, N is the number of grid cells in the region and $\bar{x}$ is the mean value over all grid cells in the region.

These values are presented using a Taylor diagram, a polar plot where the distance from the origin shows the normalised standard deviation (i.e. the ratio of model to observed standard deviation) and the cosine of the polar angles is the correlation coefficient. The observational value is at the point (1,0), marked with a star, and the distance from each point to this shows the root mean square difference between the model and observation at each point in the region (Jolliff et al., 2009). Thus the Taylor diagram gives a summary of the ability of the model to capture spatial variation: the closer the marker for each region is to the star at (1,0) the better the match between model and observation spatial distribution for that region.

For variables where sufficient observations were available, the change over time for each spatial region was calculated for model and observations. The time period for comparison varied depending on the available observations, but was at least two decades. The annual cycle was first removed from the data by seasonal decomposition, then linear regression was used to find the rate of change of the long-term trend. The tools used for this analysis were the “seasonal_decompose” method from the Python statsmodels package and the “linregress” method from scipy.stats. Where a statistically significant trend was found (p<0.01) for the model and/or observation timeseries this is shown in a table for each variable.

3.3 Validation outcome

3.3.1 Surface dissolved oxygen

The model mean surface oxygen for 1980 to 2014 was compared to the North Sea Biogeochemical Climatology. The model captures some of the spatial variability seen in the observations, for example higher values off East Anglia and in the far north, lower values in the southernmost North Sea and to the west (Figure 3.4). However, the model does not show high values in the Irish Sea or off the Norwegian coast. The model standard deviation is within about 20% of that observed in most regions, but variability is somewhat higher than observed in Northern Ireland, and much lower in Wales offshore (Figure 3.5). Model-observation correlation is about 0.5 for the UK EEZ as a whole, with Northern Ireland and England inshore having the highest correlation.

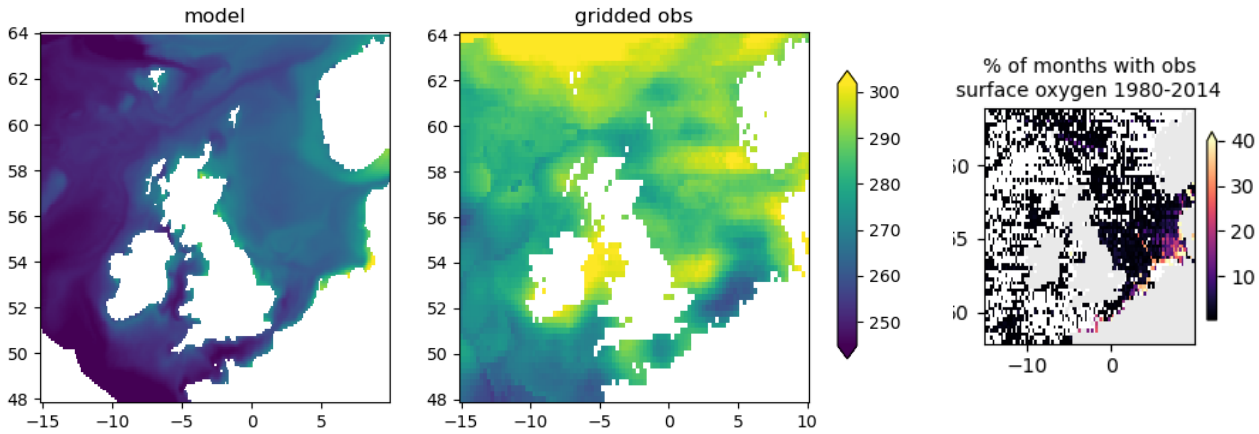

Figure 3.4 Mean surface oxygen (mmol m^{-3}) from the POLCOMS-ERSEM model (left) and the NSBC observation-based climatology (right). The panel on the far right shows the location of observations used to create the NSBC climatology.

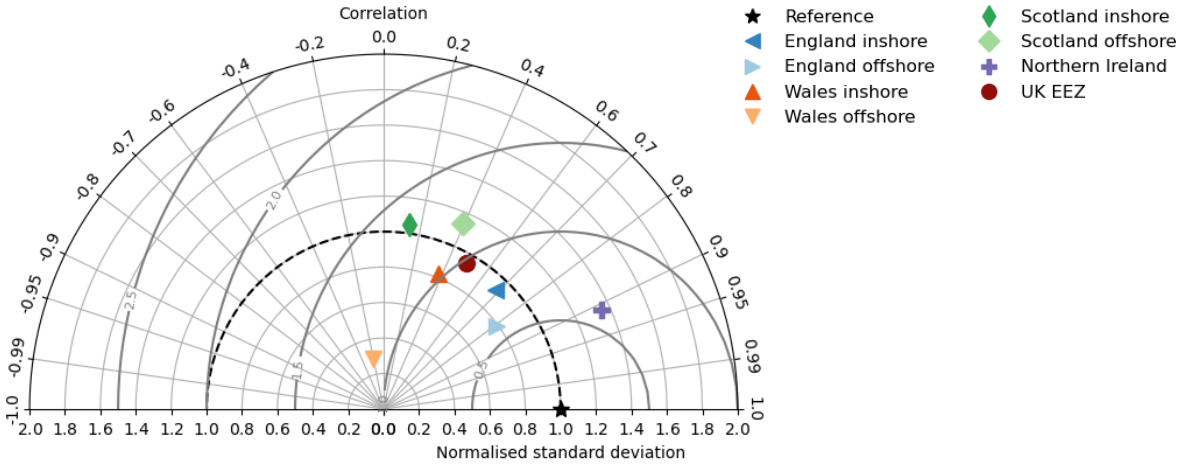

Figure 3.5 Taylor diagram for surface dissolved oxygen, summarising the spatial match between the POLCOMS-ERSEM model outputs and values from the NSBC observation-based climatology, for UK national marine areas. Values closer to the reference point show better agreement. For information about how the diagram was created see section 3.2.2.

The model gives a falling trend over time, consistent with observations, however it is smaller than observed, particularly in Scotland (Table 3.2).

Table 3.2 Temporal trend in surface oxygen (mmol m^{-3} per decade) for national regions and the UK EEZ, 1980-2014. "-" indicates that any trend was not statistically significant; "n/a" means that there was too little observational data available to analyse.

	UK EEZ	England	Wales	Scotland	N. Ireland
POLCOMS-ERSEM model	-0.45	-0.46	-	-0.47	-
NSBC observations	-3.58	-1.67	-	-3.01	n/a

Overall, the model captures some of the spatial variation and underpredicts the small decrease in oxygen over a multidecadal period. Confidence is assessed as moderate for England and the EEZ as a

whole, lower for Scotland and Wales and with limited data making assessment difficult for Northern Ireland.

3.3.2 Bottom dissolved oxygen

The model mean bottom level oxygen for 1980 to 2014 was compared to the North Sea Biogeochemical Climatology. The model captures some of the spatial variability seen in the observations, for example higher values off East Anglia and in the Irish Sea, lower values in the southernmost North Sea and to the west (Figure 3.6). Values are lower than observed, especially in the far north and the west. The model and observed standard deviation are similar in most regions, but larger for England offshore and for Scotland, especially offshore (Figure 3.7). Inshore waters in Wales and England have model-observation correlation of 0.8 or above, but the correlation is weaker elsewhere.

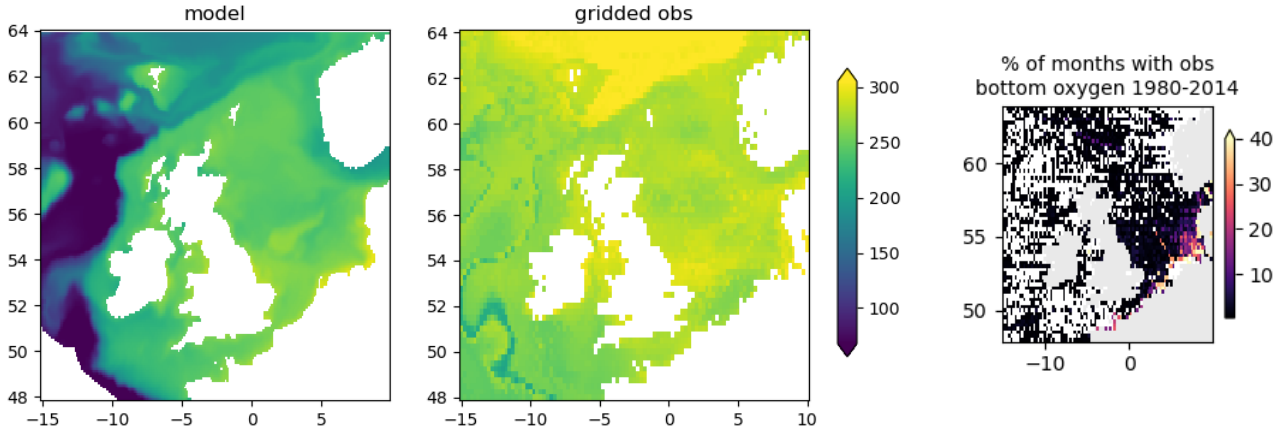

Figure 3.6 Mean bottom-level dissolved oxygen (mmol m^{-3}) from the POLCOMS-ERSEM model (left) and the NSBC observation-based climatology (right). The panel on the far right shows the location of observations used to create the NSBC climatology.

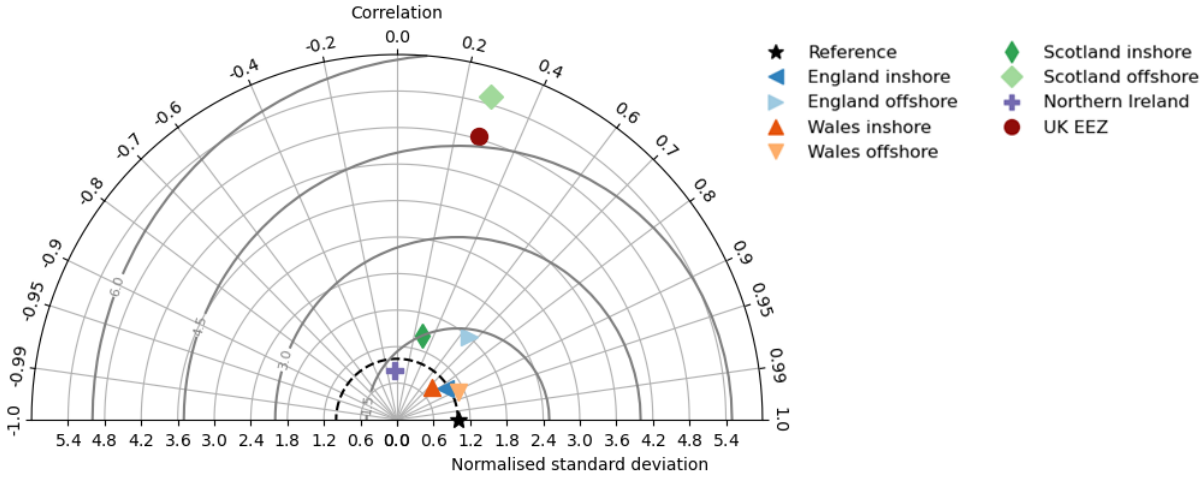

Figure 3.7 Taylor diagram for bottom-level dissolved oxygen, summarising the spatial match between the POLCOMS-ERSEM model outputs and values from the NSBC observation-based climatology, for UK national marine areas. Values closer to the reference point show better agreement. For information about how the diagram was created see section 3.2.2.

There is quite good agreement on trend over time everywhere there is sufficient observational data to assess it (Table 3.3). The trend is negative everywhere except Northern Ireland, which has no significant trend. The trend for England is lower than observed, but comparable to observations for the UK EEZ overall, influenced by the much greater trend in Scotland.

Table 3.3 Temporal trend in bottom level oxygen (mmol m^{-3} per decade) for national regions and the UK EEZ, 1980-2014. "-" indicates that any trend was not statistically significant; "n/a" means that there was too little observational data available to analyse.

	UK EEZ	England	Wales	Scotland	N. Ireland
POLCOMS-ERSEM model	-4.9	-0.76	-0.23	-7.0	-
NSBC observations	-4.3	-2.82	n/a	-6.6	n/a

Overall, Scotland shows good temporal agreement with observations but weaker spatial agreement, especially in offshore areas. The reverse is true for England, where there is relatively good spatial agreement but a weaker trend than observed. Confidence is assessed as moderate for both nations. There is too little observational data to give a confidence score for Northern Ireland; Wales does not have sufficient observational data to derive a temporal trend but, given the good spatial agreement, confidence is assessed as moderate.

3.3.3 Surface sea water potential temperature

The model mean sea surface temperature for 1980 to 2014 was compared to the North Sea Biogeochemical Climatology and to the larger dataset in the Hydrographic Climatology of the North Sea and Surrounding Regions. The range of temperatures is lower than observed, as can be seen from the location inside the radius 1 circle on the Taylor diagram (Figure 3.9) and the smaller range of values on the climatology plot (Figure 3.8). Spatial variability is well captured, however, with lower values in the northern North Sea and the north of Ireland, higher values in the south-west and near the coast of continental Europe. Spatial correlation is 0.7 or higher in most regions, the exception being Northern Ireland, where in-region differences are not captured.

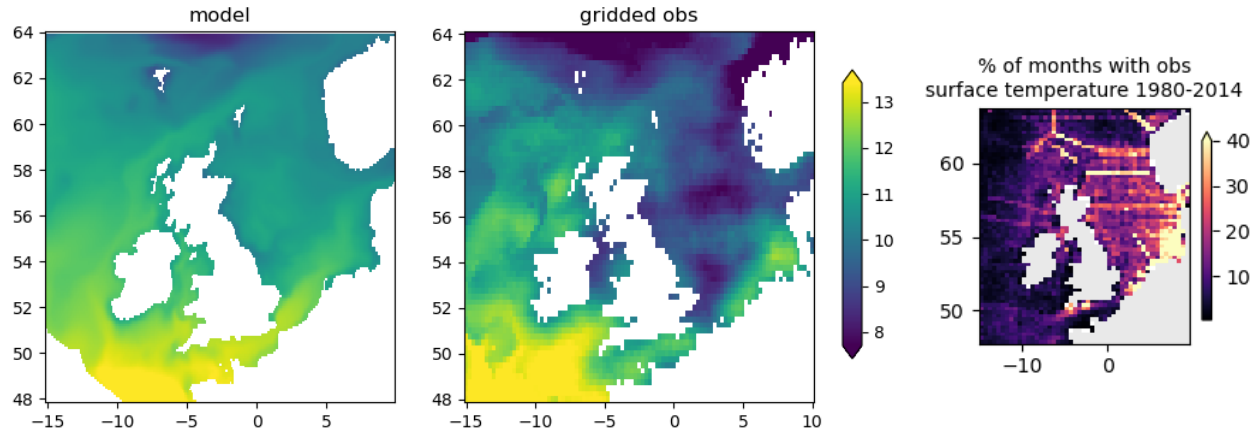

Figure 3.8 Mean surface temperature (°C) from the POLCOMS-ERSEM model (left) and the NSBC observation-based climatology (right). The panel on the far right shows the location of observations used to create the NSBC climatology.

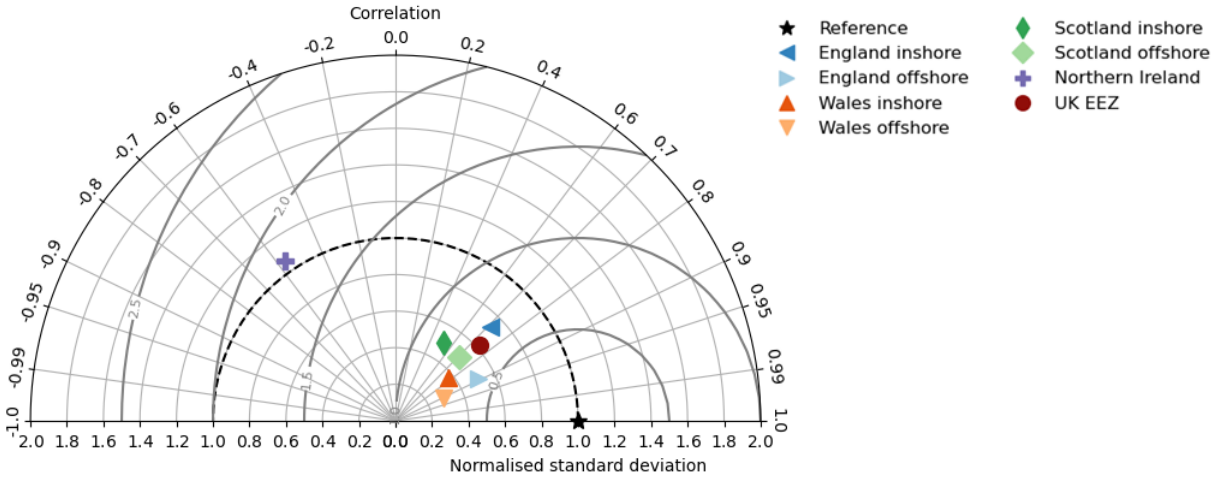

Figure 3.9 Taylor diagram for surface temperature, summarising the spatial match between the POLCOMS-ERSEM model outputs and values from the NSBC observation-based climatology, for UK national marine areas. Values closer to the reference point show better agreement. For information about how the diagram was created see section 3.2.2.

Satellite observations are available for 1982-2021: this slightly more recent climatology shows a similar pattern of spatial agreement (Figure 3.10).

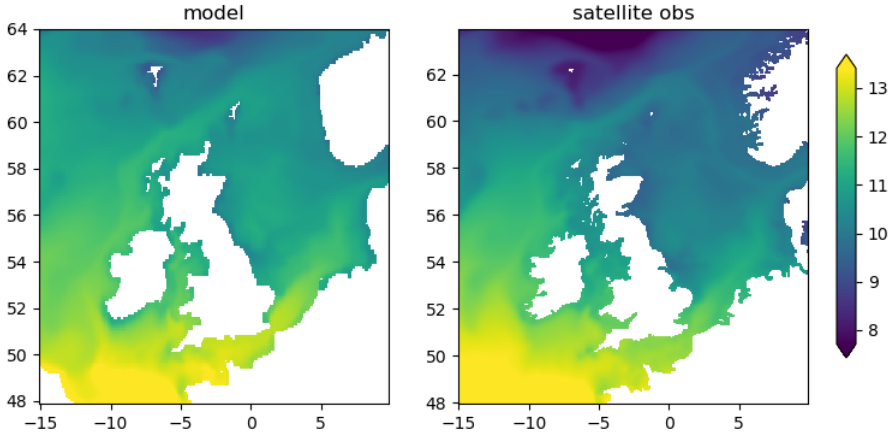

Figure 3.10 Mean sea surface temperature (°C) for 1982-2021, from the POLCOMS-ERSEM model outputs (left) and satellite observations (right).

Modelled temporal trends for 1980-2014 are smaller than observed (Table 3.4). In fact, the model temperatures are fairly static for most of this period but show a sharper rise for years since 2014 (Figure 3.11). Satellite estimates, which are available for 1982-2022, show a similar pattern of relatively static phases and periods of faster increase, though with the rise occurring some years earlier. Given that climate models aim to capture general trends rather than year-to-year agreement, this can be considered as good performance.

Table 3.4 Temporal trend in sea surface temperature (°C per decade) for national regions and the UK EEZ, 1980-2014. "-" indicates that any trend was not statistically significant; "n/a" means that there was too little observational data available to analyse.

	UK EEZ	England	Wales	Scotland	N. Ireland
POLCOMS-ERSEM model 1980-2014	0.03	0.06	-	-	-
KNSC observations 1980-2014	0.23	0.19	-0.17	0.37	-0.19
POLCOMS-ERSEM model 1982-2021	0.13	0.17	0.14	0.11	0.13
satellite observations 1982-2021	0.26	0.30	0.27	0.24	0.24

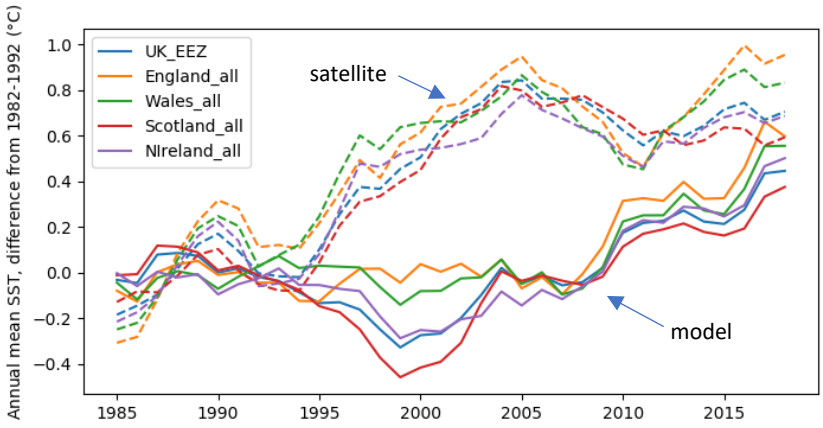

Figure 3.11 Smoothed annual mean sea surface temperature anomaly (°C) for UK national marine areas, from the POLCOMS-ERSEM model (solid lines) and satellite observations (dashed line). The values have been smoothed with a 5-year kernel to show long-term trends. The anomaly is the difference from the mean value for 1982-1992.

Overall, the good spatial agreement and rising trends mean that confidence is assessed as strong everywhere except Northern Ireland. However, it should be noted that the temperature rise is lower than both satellite and in situ observations, so the projections should be considered at the low end of the possible range of climate change. This is consistent with the parent global model having a temperature response in the low to moderate end of the CMIP5 range.

3.3.4 Bottom sea water potential temperature

The model mean bottom level temperature for 1980 to 2014 was compared to the North Sea Biogeochemical Climatology and to the larger dataset in the Hydrographic Climatology of the North Sea and Surrounding Regions. The observational temperatures are somewhat lower than observed, on average, but spatial patterns are well reproduced: highest in the English Channel and southern North Sea, lower in the deeper waters of the northern North Sea and off-shelf (Figure 3.12). The model outputs have lower variability than observed (points are mainly inside the radius 1 line on the

Taylor diagram (Figure 3.13). Northern Ireland and Wales are least well represented, with low correlations in both cases.

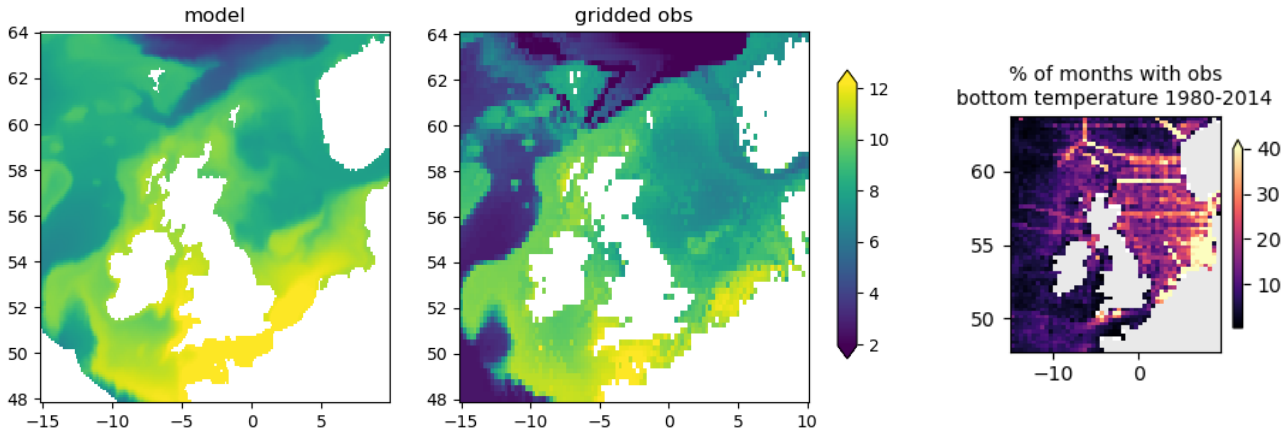

Figure 3.12 Mean bottom-level temperature (°C) from the POLCOMS-ERSEM model (left) and the NSBC observation-based climatology (right). The panel on the far right shows the location of observations used to create the NSBC climatology.

Figure 3.13 Taylor diagram for bottom-level temperature, summarising the spatial match between

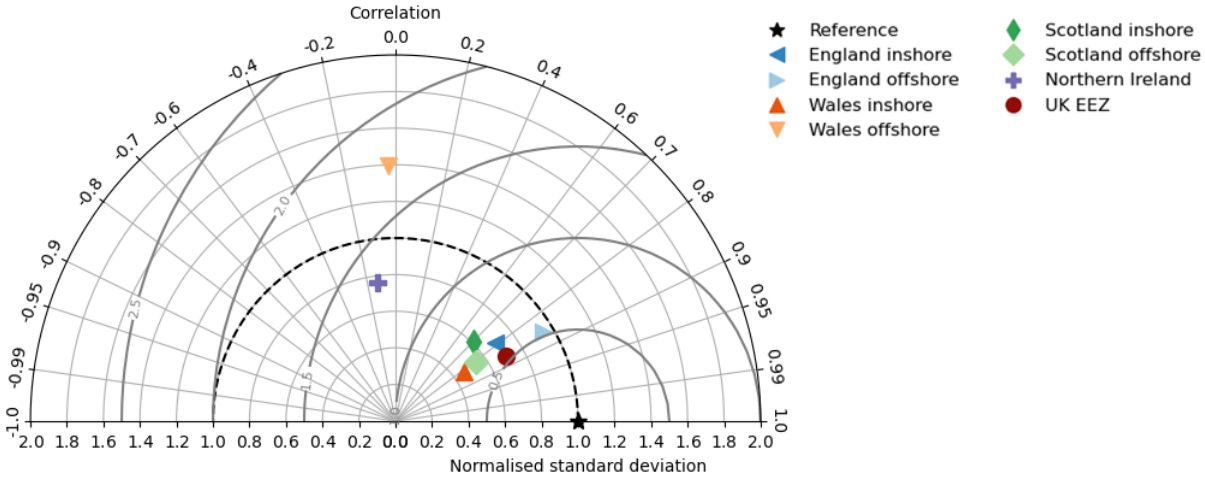

the POLCOMS-ERSEM model outputs and values from the NSBC observation-based climatology, for UK national marine areas. Values closer to the reference point show better agreement. For information about how the diagram was created see section 3.2.2.

Trends over time are smaller than for sea surface temperature, and there is no significant change for much of the region (Table 3.5). Model outputs for Scotland are negative (falling temperatures) whereas observations show a rise, and this difference is also seen for the UK EEZ as a whole.

Table 3.5 Temporal trend in bottom level temperature (°C per decade) for national regions and the UK EEZ, 1980-2014. "-" indicates that any trend was not statistically significant.

	UK EEZ	England	Wales	Scotland	N. Ireland
POLCOMS-ERSEM model	-0.05	-	-	-0.08	-

KNSC obs	0.11	-	-	0.50	-

Overall, there is good representation of spatial variability, except for Wales and Northern Ireland, but poor representation of temporal trends. Confidence is assessed as moderate for England, weak elsewhere and for the UK as a whole.

3.3.5 Surface sea water salinity

The model mean sea surface salinity for 1980 to 2014 was compared to the North Sea Biogeochemical Climatology and to the larger dataset in the Hydrographic Climatology of the North Sea and Surrounding Regions. Spatial patterns are in good agreement, though the model salinity is lower than observed for deep waters (Figure 3.14). Variability within regions is higher in the model than in observations (points are outside the radius 1 circle on the Taylor diagram (Figure 3.15) but spatial correlation is good everywhere (weakest for Northern Ireland).

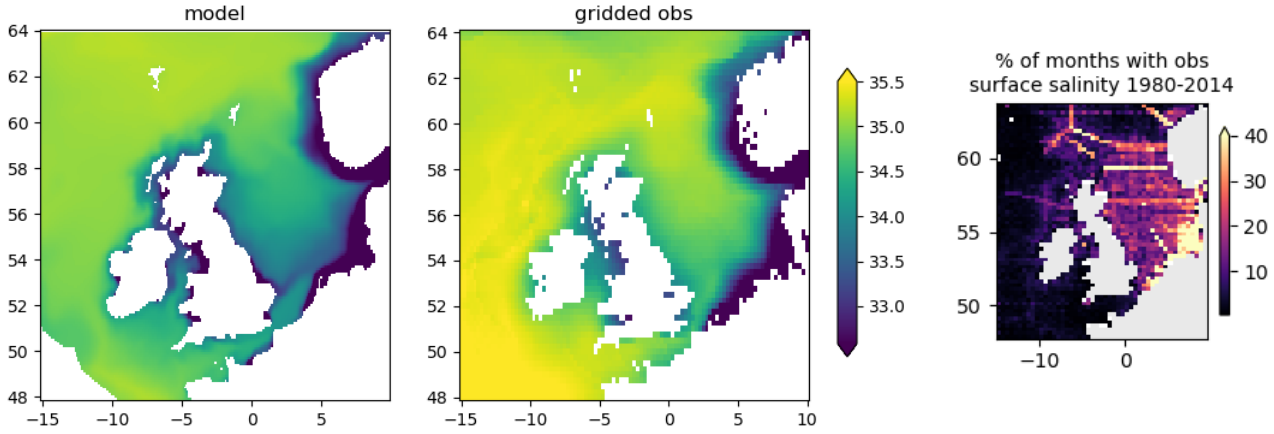

Figure 3.14 Mean surface salinity (psu) from the POLCOMS-ERSEM model (left) and the NSBC observation-based climatology (right). The panel on the far right shows the location of observations used to create the NSBC climatology.

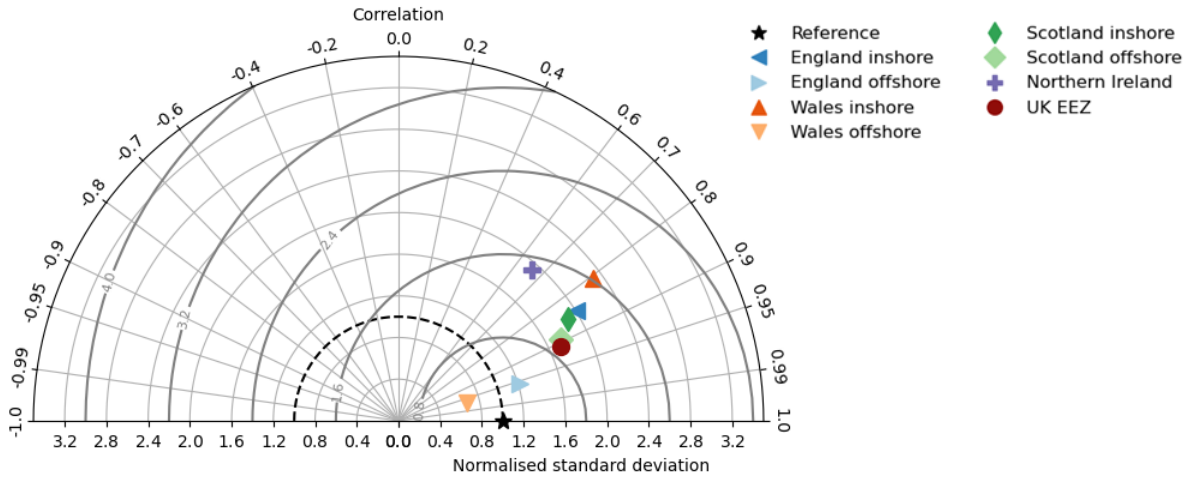

Figure 3.15 Taylor diagram for surface salinity, summarising the spatial match between the POLCOMS-ERSEM model outputs and values from the NSBC observation-based climatology, for UK

national marine areas. Values closer to the reference point show better agreement. For information about how the diagram was created see section 3.2.2.

Model values show a slow decrease over time, of about 0.2 psu per decade, whereas observations show no change or a small increase (Table 3.6).

Table 3.6 Temporal trend in sea surface salinity (psu per decade) for national regions and the UK EEZ, 1980-2014. "-" indicates that any trend was not statistically significant.

	UK EEZ	England	Wales	Scotland	N. Ireland
POLCOMS-ERSEM model	-0.17	-0.19	-0.17	-0.16	-0.19
KNSC obs	0.04	-	-	0.02	-

The discrepancy in the direction of trend means that the confidence is assessed as moderate in spite of the good spatial agreement. For Wales and England there is better agreement on trend, so these areas are assessed as strong confidence.

3.3.6 Bottom sea water salinity

The model mean bottom level salinity for 1980 to 2014 was compared to the North Sea Biogeochemical Climatology and to the larger dataset in the Hydrographic Climatology of the North Sea and Surrounding Regions. Spatial agreement is particularly good for offshore areas of England and Wales, with correlation 0.95 (Figure 3.17) and similar patterns visible in spatial plots (Figure 3.16), though observed values are generally higher than the model outputs. Inshore areas of Scotland and England also show good correlation, but correlation is poor for offshore areas of Scotland and for Northern Ireland.

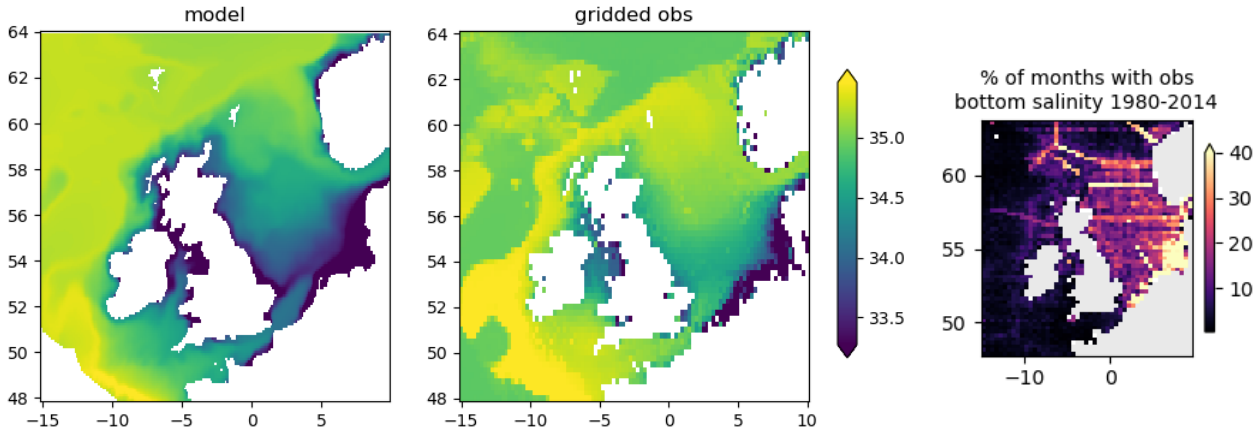

Figure 3.16 Mean bottom-level salinity (psu) from the POLCOMS-ERSEM model (left) and the NSBC observation-based climatology (right). The panel on the far right shows the location of observations used to create the NSBC climatology.

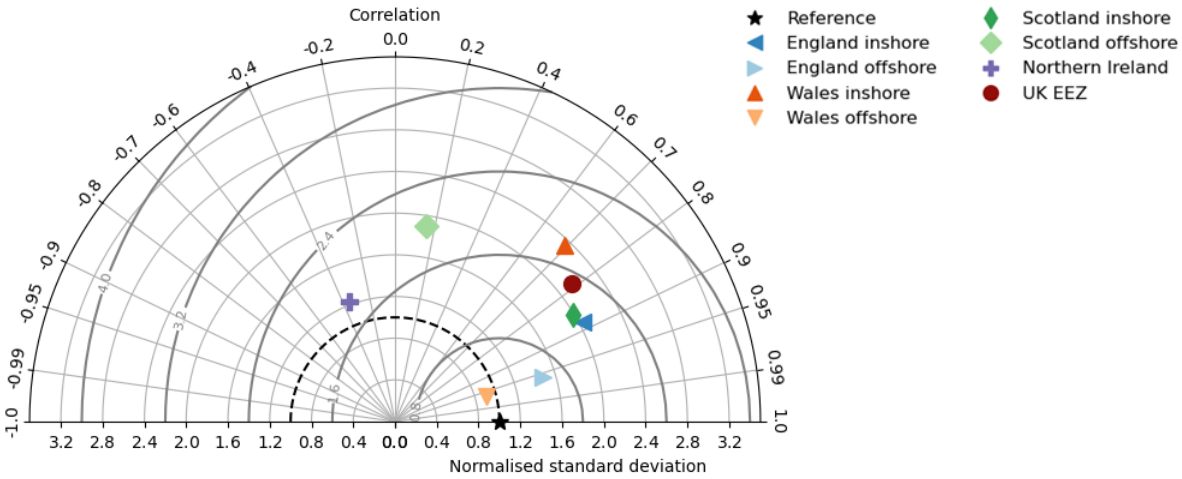

Figure 3.17 Taylor diagram for bottom-level salinity, summarising the spatial match between the POLCOMS-ERSEM model outputs and values from the NSBC observation-based climatology, for UK national marine areas. Values closer to the reference point show better agreement. For information about how the diagram was created see section 3.2.2.

As seen with surface salinity, the temporal trend for bottom level salinity is to increase in the observations but decrease in the model outputs (Table 3.7).

Table 3.7 Trend in bottom level salinity (psu per decade) for national regions and the UK EEZ, 1980-2014. "-" indicates that any trend was not statistically significant.

	UK EEZ	England	Wales	Scotland	N. Ireland
POLCOMS-ERSEM model	-0.14	-0.18	-0.17	-0.12	-0.19
KNSC obs	0.08	0.04	-	0.07	0.07

There is poor agreement in either spatial or temporal variation for all areas and so the confidence is assessed as weak. However, the good spatial agreement for England and Wales should be noted, and the variation within these areas may be reliable even if trends are uncertain.

3.3.7 Surface sea water pH

Surface pH was compared to observations from the GLODAP database. These are much sparser than those available for oxygen, temperature and salinity (Figure 3.18, right-hand panel), but some assessment can be made. Spatial variation in the model is in rough agreement with the GLODAP gridded climatology, with lowest values in the shallow waters of the southern North Sea, English Channel and Irish Sea (Figure 3.18). The high model values on coast of Denmark and Germany are not seen in observations. The model also has high values in the far north but observations are missing there – the gridded climatology is interpolated from other areas and may not be reliable. The Taylor diagram shows negative correlation for Wales and 0 for England, but these are likely to be affected by the lack of observations in the western part of the region.

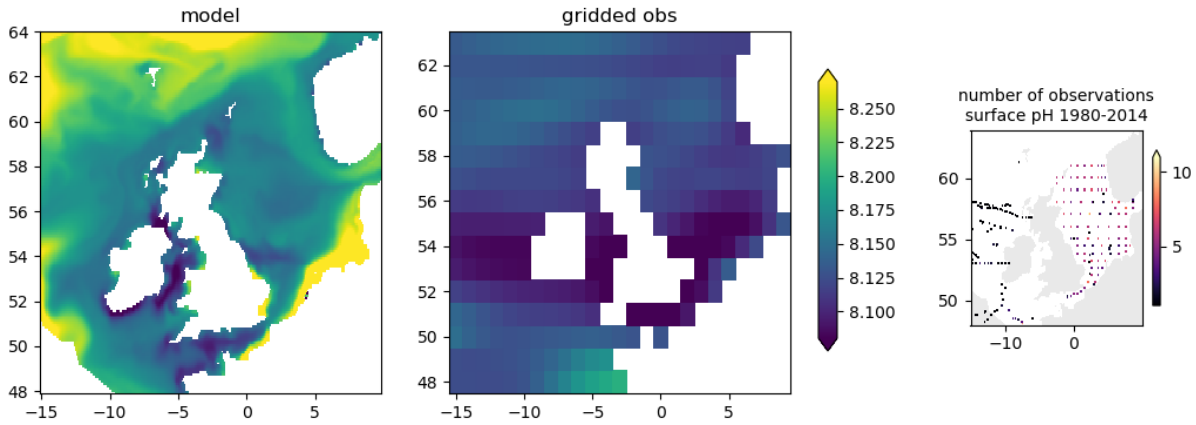

Figure 3.18 Mean surface pH from the POLCOMS-ERSEM model (left) and the GLODAP observation-based climatology (right). The panel on the far right shows the location of observations used to create the GLODAP gridded climatology.

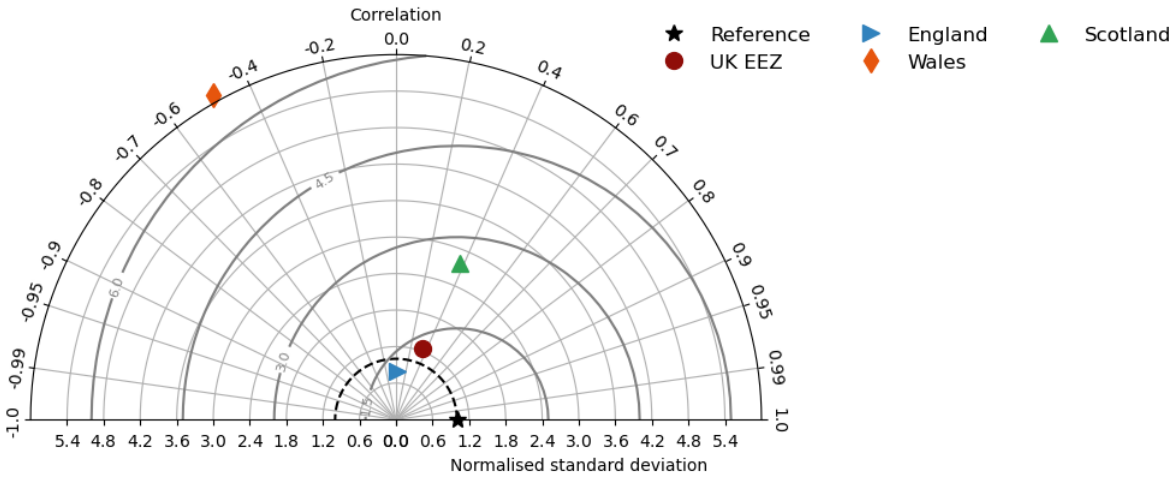

Figure 3.19 Taylor diagram for surface pH, summarising the spatial match between the POLCOMS-ERSEM model outputs and values from the GLODAP observation-based gridded climatology, for UK national marine areas. Values closer to the reference point show better agreement. For information about how the diagram was created see section 3.2.2.

The model values show surface pH falling by 0.012 units per decade over the UK EEZ. The GLODAP dataset has insufficient observations to calculate a trend. A global product which uses a machine learning approach to extend the coverage (https://doi.org/10.48670/moi-00047) gives a fall of about 0.016 units per decade for the seas around the UK. OSPAR's intermediate assessment (OSPAR, 2017) cites values of 0.02 units per decade in the OSPAR Maritime area, with 0.035+/-0.014 units per decade in the Greater North Sea (Ostle et al., 2016).

There is enough information on spatial variation and trend to assess moderate confidence for the UK EEZ and Scotland, weak for England; however, there is too little evidence for Wales and Northern Ireland. It should be noted that trends in surface pH are somewhat smaller than observed: as for sea surface temperature, the projections should be considered at the low end of the possible range of climate change/ocean acidification.

3.3.8 Bottom sea water pH

Bottom level pH was compared to observations from the GLODAP database. The assessment is similar to that for surface pH, above: some correspondence in patterns of variation where observations are available, but limited observations for the north and west of the region (Figure 3.20, Figure 3.21). No observational data on temporal trends are available.

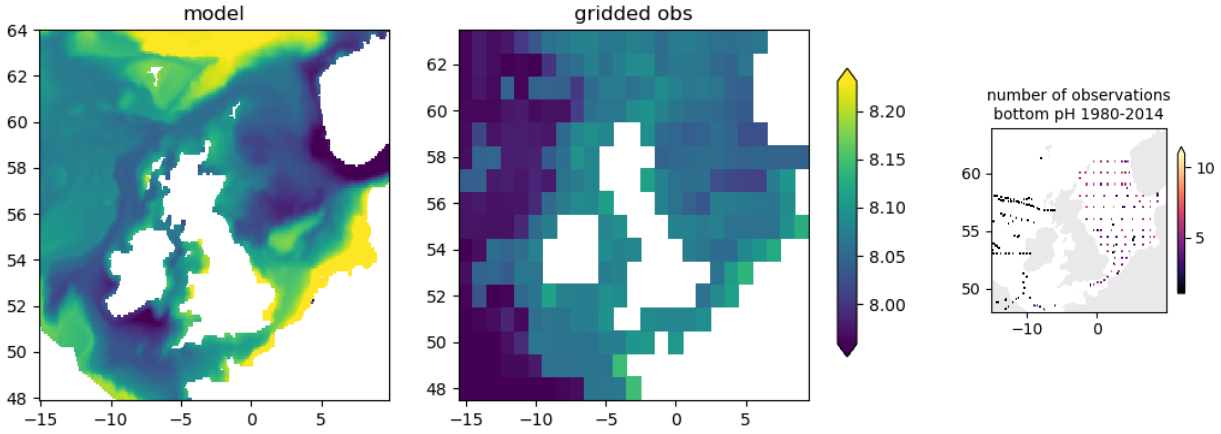

Figure 3.20 Mean bottom-level pH from the POLCOMS-ERSEM model (left) and the GLODAP observation-based climatology (right). The panel on the far right shows the location of observations used to create the GLODAP gridded climatology.

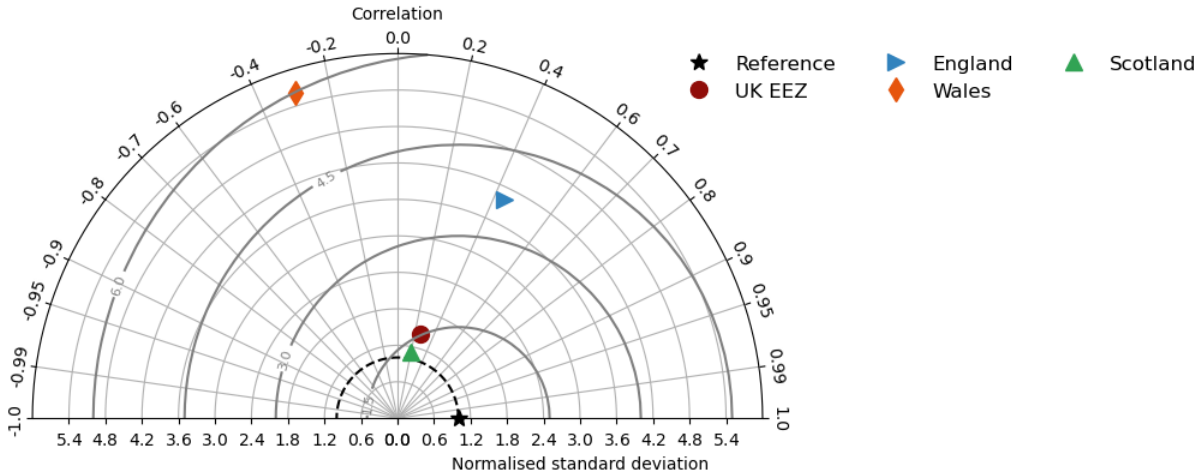

Figure 3.21 Taylor diagram for bottom-level pH, summarising the spatial match between the POLCOMS-ERSEM model outputs and values from the GLODAP observation-based gridded climatology, for UK national marine areas. Values closer to the reference point show better agreement. For information about how the diagram was created see section 3.2.2.

Given the similarity to surface pH, the confidence assessment is the same: moderate for the UK EEZ and Scotland and weak for England; too little evidence for Wales and Northern Ireland. However in deeper water the correspondence between surface and bottom levels is likely to be less strong and the confidence should be treated as uncertain.

3.3.9 Surface saturation state of aragonite

Aragonite saturation state at the surface was compared to observations from the GLODAP database. It is calculated from the same measurements as pH and so the distribution of observations can be assumed the to be the same (Figure 3.22, right-hand panel). Although there is some correspondence in spatial variation between model and observations, with lowest values in the English Channel, Irish Sea and southern North Sea (Figure 3.22) , correlation is weak everywhere (Figure 3.23).

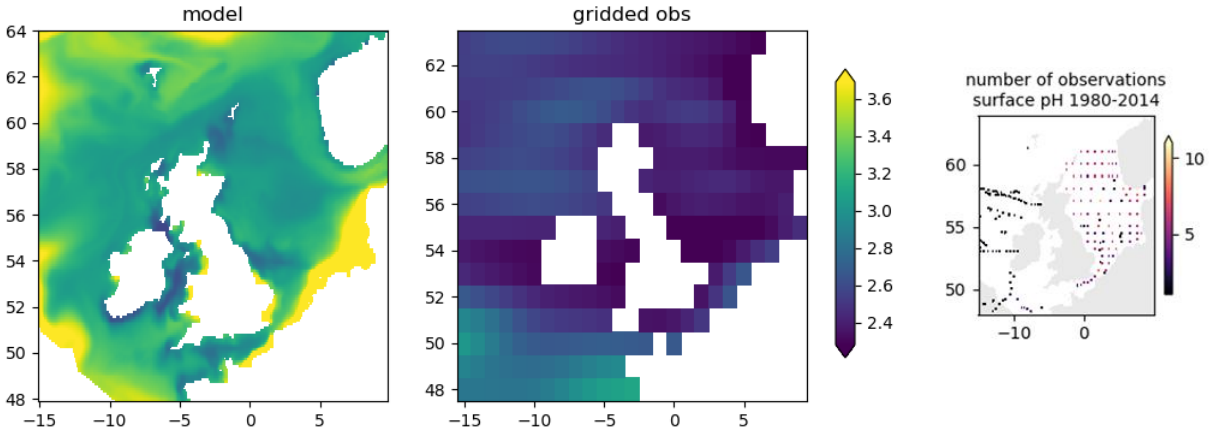

Figure 3.22 Mean surface aragonite saturation state from the POLCOMS-ERSEM model (left) and the GLODAP observation-based climatology (right). The panel on the far right shows the location of observations used to create the GLODAP gridded climatology.

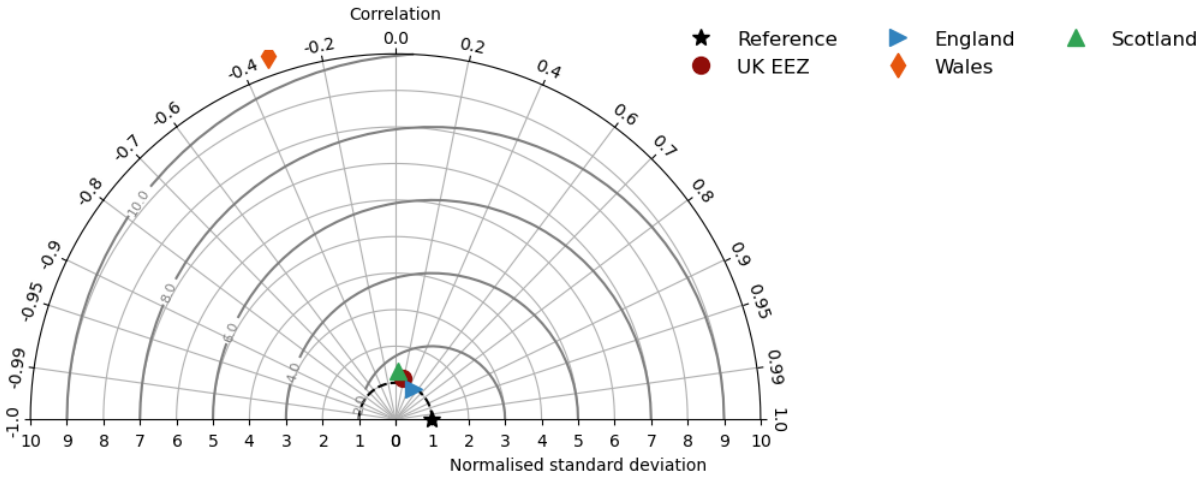

Figure 3.23 Taylor diagram for surface aragonite saturation state, summarising the spatial match between the POLCOMS-ERSEM model outputs and values from the GLODAP observation-based gridded climatology, for UK national marine areas. Values closer to the reference point show better agreement. For information about how the diagram was created see section 3.2.2.

Observational data on was insufficient to evaluate temporal trends in pH.

Overall, the confidence is assessed as weak, but on a low evidence base. Given the lack of observations in Wales and Northern Ireland, the confidence for these areas is uncertain.

3.3.10 Bottom saturation state of aragonite

Aragonite saturation state at the bottom level was compared to observations from the GLODAP database. It is calculated from the same measurements as pH and so the distribution of observations can be assumed the to be the same. Spatial correlation is 0.7 or better for England and Scotland, showing broad agreement overall (Figure 3.25). Some correspondence can also be seen in the spatial plots: highest values in the southern North Sea and western Scotland, lower for the northern North Sea (Figure 3.24). Agreement is worse for Wales, but the observation-based climatology relies on extrapolation from neighbouring areas so is unreliable. No observational data on temporal trends are available.

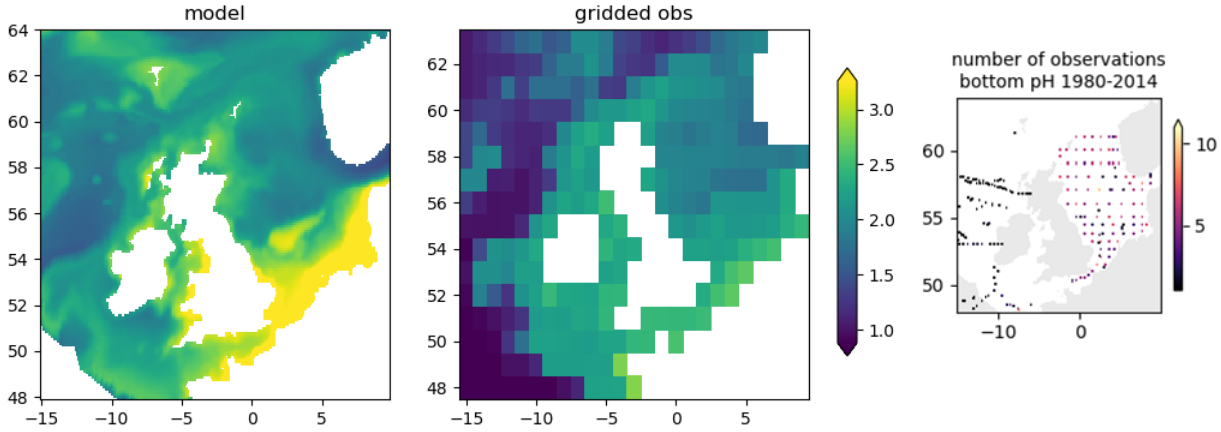

Figure 3.24 Mean bottom-level aragonite saturation state from the POLCOMS-ERSEM model (left) and the GLODAP observation-based climatology (right). The panel on the far right shows the location of observations used to create the GLODAP gridded climatology.

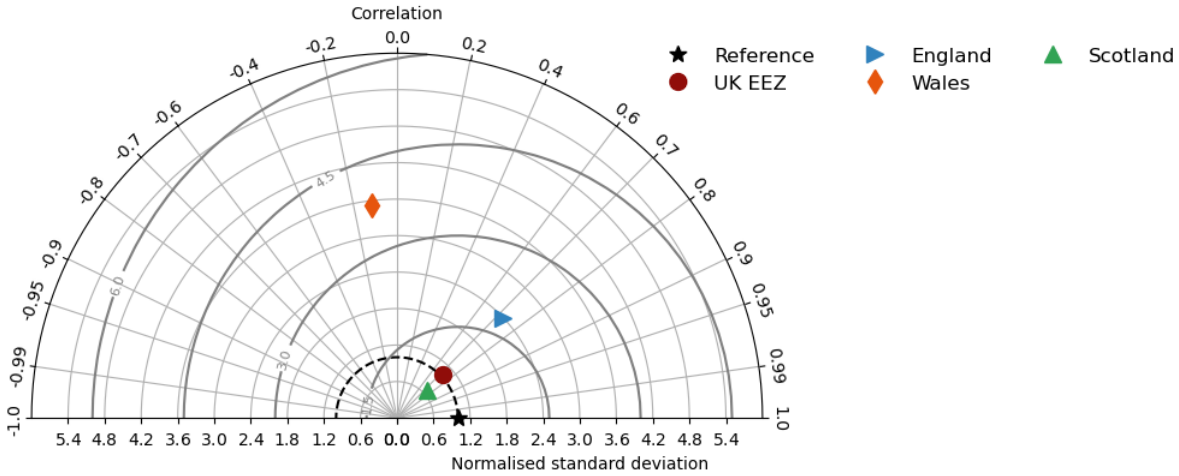

Figure 3.25 Taylor diagram for bottom-level aragonite saturation state, summarising the spatial match between the POLCOMS-ERSEM model outputs and values from the GLODAP observation-based gridded climatology, for UK national marine areas. Values closer to the reference point show better agreement. For information about how the diagram was created see section 3.2.2.

Overall the confidence is assessed as moderate, but on a low evidence base. Given the lack of observations in Wales and Northern Ireland, the confidence for these areas is uncertain.

3.3.11 Net primary production

Water-column total net primary production was used as an input to the meta-analysis. Comparison to estimates derived from ocean colour satellite data is given here, however the satellite product is optimised for the open ocean and may not be reliable in coastal and shallow seas. Comparison to estimates of gross primary production for the North Sea is therefore provided as well.

Net primary production was compared to satellite-based estimates from a global product (Copernicus-GlobColour, https://doi.org/10.48670/moi-00281). Plots of model and satellite average values for net primary production show good agreement on spatial patterns, though model-derived values are higher and show less variability than satellite estimates (Figure 3.26). Production is highest in coastal areas, lower in central areas of the Irish Sea, western English Channel and northern North Sea.

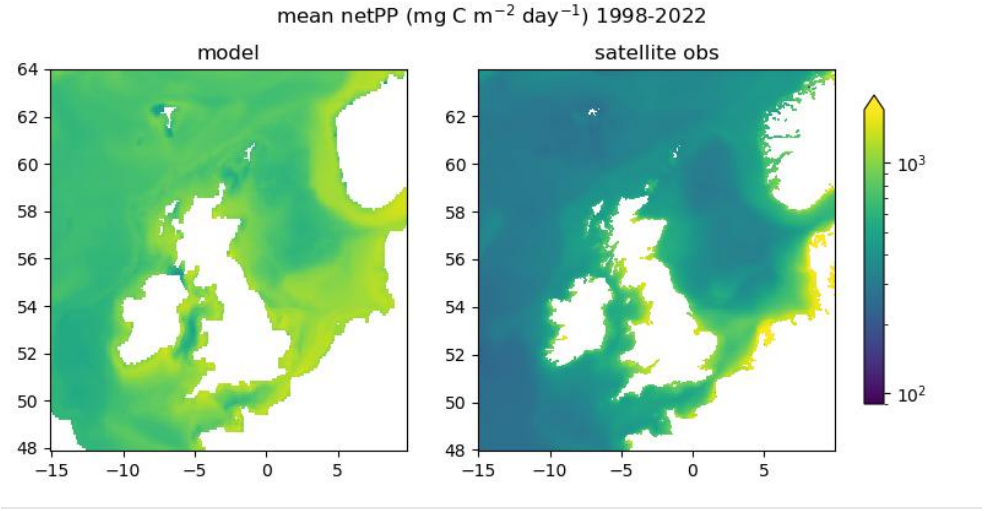

Figure 3.26 Mean net primary production (mg C m^{-2} day^{-1}) for 1998-2022, from the POLCOMS-ERSEM model outputs (left) and derived from ocean-colour satellite observations (right).

There is good agreement on the direction of temporal trends: falling production in Scotland and for the UK EEZ as a whole, rising in Northern Ireland and little change for England and Wales (Table 3.8). The modelled fall for Scotland and the EEZ is smaller than the satellite estimates, but given the uncertainty in the satellite values the difference is not large.

Table 3.8 Temporal trend in column total net primary production (mg C m^{-2} day^{-1} per decade) for national regions and the UK EEZ, 1989-2022. "-" indicates that any trend was not statistically significant.

	UK EEZ	England	Wales	Scotland	N. Ireland
POLCOMS-ERSEM model	-10	-	9	-15	16
Satellite-derived	-21	-	-	-22	14

Model outputs for column total gross primary production were compared to a published study of spatial variation and trends for the North Sea (Capuzzo et al., 2018). This study used all available in situ measurements of chlorophyll and light attenuation for 1988-2013. Capuzzo et al. divided the region into six hydrodynamic zones (Figure 3.27) and calculated the mean productivity and trend over time in each zone. Their Table 1 is reproduced below (Table 3.9), with the corresponding model values shown in italics below each number. Slope and standard error are only given where the trend in annual primary production is significant (p<0.01, denoted by **).

The model values are consistently larger than the observation-based values but the spatial variation is in good agreement, as can be seen in the similarity in the percentage of production in each of the six regions. For both datasets the region of freshwater influence and the transitional east zone are highly productive, the seasonally stratified zone less so (see also Figure 3.28). Model-observation difference is highest for the permanently mixed area, for which the model outputs have higher productivity than the observation-based dataset.

Capuzzo et al. found an overall decrease in gross primary production for the North Sea, with the strongest trends in the transitional zones between seasonally stratified and permanently mixed zones. Elsewhere the trend was not statistically significant. The trend in the model outputs is significant for the western transitional zone, the seasonally stratified zone and for the North Sea as a whole (Table 3.9 and Figure 3.28). Trends in the model outputs are smaller than in the observation-based dataset, but agree on the declining trend. We conclude that there is agreement between the model and observations on a reduction in primary production, though the size and location of the change differ.

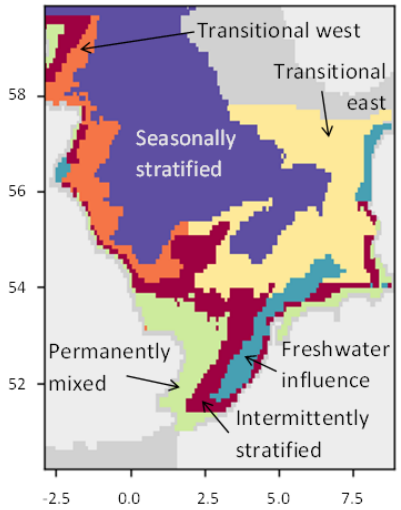

Figure 3.27 Hydrodynamic zones of the North Sea, as used by Capuzzo et al. (2018).

Table 3.9 G ross primary production for different areas of the North Sea estimated by Capuzzo et al. (2018) and by the POLCOMS-ERSEM model. In each box of the table the top number comes from Capuzzo et al. (their Table 1), the lower one, in italics, from the model. PP = column total gross primary production, SE = standard error. ** denotes a statistically significant trend (p<0.01).

Region	PP (g C m^{-2} $year^{-1}$)		Area PP (10^{12} g C $year^{-1}$)		Annual change in PP (g C m^{-2} $year^{-1}$)			
	mean	SE	Mean (%)	SE	r^2	*p*	slope	SE
Seasonally stratified	200 *382*	15 *20*	34.9 (36) *65.7 (35)*	2.75 *3.42*	0.091 *0.722*	0.134 *0.000***	 -2.21	 0.28
Transitional East	354 *510*	54 *23*	27.6 (28) *42.1 (23)*	4.24 *1.87*	0.299 *0.086*	.0039** *0.145*	-19.78	6.19
Transitional West	187 *486*	15 *24*	5.8 (6) *16.4 (9)*	0.47 *0.80*	0.278 *0.597*	.0057** *0.000***	-5.38 -1.78	1.77 0.30
Intermittently stratified	268 *526*	20 *22*	16.3 (17) *29 (16)*	1.24 *1.20*	0.001 *0.059*	0.884 *0.231*		
Permanently mixed	82 *551*	7 *22*	4.0 (4) *20.6 (11)*	0.35 *0.81*	0.128 *0.051*	.073 *0.268*		
Freshwater influence	382 *578*	28 *24*	8.7 (9) *13.1 (7)*	0.65 *0.54*	0.001 *0.000*	.903 *0.970*		
North Sea	234 *463*	17 *21*	97.34 (100) *186.9 (100)*	6.92 *8.5*	0.261 *0.591*	.0076** *0.000***	-5.67 -1.27	1.94 0.22

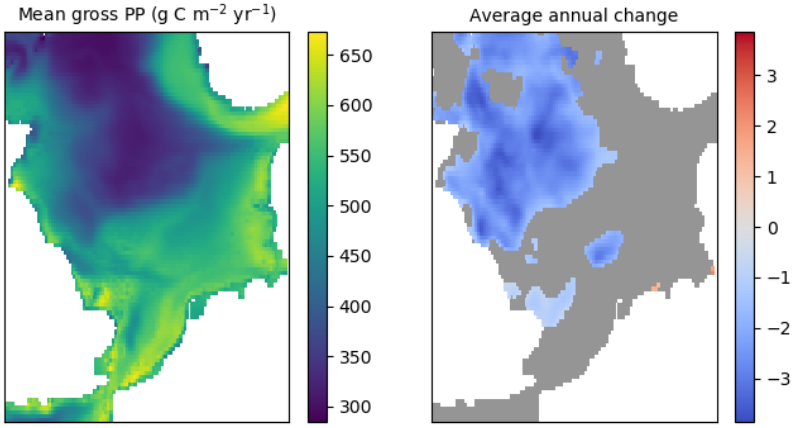

Figure 3.28 Gross primary production for the North Sea, from POLCOMS-ERSEM model outputs. The left-hand panel shows the mean value for 1988-2013, the right-hand panel shows the mean annual change over the same period. Grey shading indicates no significant change (p>0.01)

Overall, the model reproduces the spatial distribution of primary production well, for both the net and gross primary production datasets. There is also agreement on the declining trend in productivity, though the trend is smaller for the model outputs than from satellite estimates, and not statistically significant in many places. Confidence is assessed as moderate for all regions.

3.3.12 Potential energy anomaly (stratification)

Potential energy anomaly is derived from the variation in density over the top 200m. This is calculated from temperature and salinity so the assessment of surface and bottom temperature and salinity gives a guide to reliability. Confidence in surface values is moderate to strong in most regions but poor representation of the observed trends at bottom levels means that confidence in potential energy anomaly is assessed as weak.

3.3.13 Surface thermal fronts

The location of thermal fronts is derived from modelled sea surface temperature data. The method used for front location has been demonstrated to have high accuracy when applied when using satellite measurements (Miller, 2009). The confidence in the model-derived dataset can therefore be assessed as the same as the confidence in sea surface temperature (section 3.3.3): weak for Northern Ireland, strong elsewhere.

3.3.14 Water column sum of phytoplankton carbon

There was insufficient observational data on phytoplankton biomass to make a direct comparison to the model outputs. Chlorophyll concentration gives an indication of phytoplankton biomass, so model outputs have been compared to chlorophyll data derived from ocean colour satellite observations.

The spatial distribution of chlorophyll shows a good match to that observed by satellite. The on-shelf values tend to be higher than satellite except close to the coasts; the high satellite values for complex waters near river mouths may be unreliable (Figure 3.29).

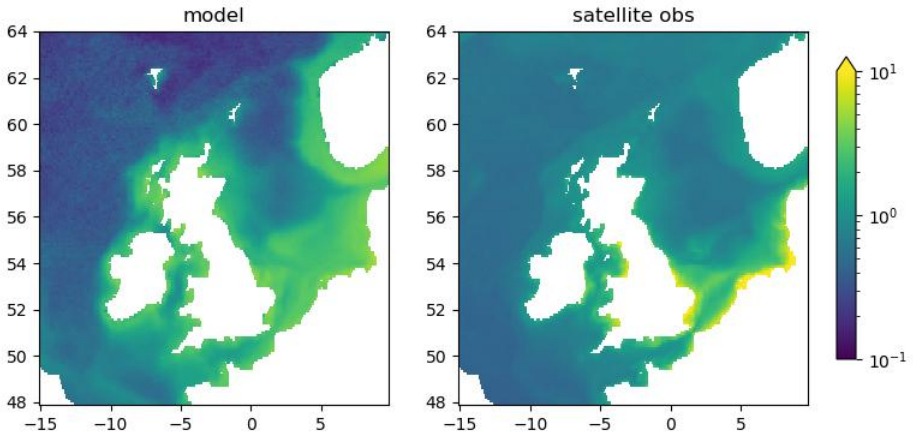

Figure 3.29 Mean surface chlorophyll concentration (mg C m^{-3}) for 1998-2021, from the POLCOMS-ERSEM model outputs (left) and derived from ocean-colour satellite observations (right).

For all areas except England, the model outputs show a falling trend in log-chlorophyll concentration over time (Figure 3.30 and Table 3.10). The satellite observations have a rising trend in England, Wales and Northern Ireland, falling in Scotland and no change overall.

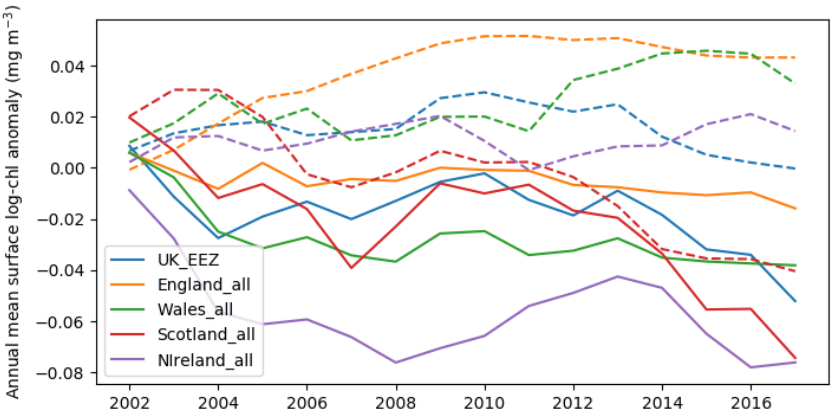

Figure 3.30 Smoothed annual mean anomaly in surface log-chlorophyll (log(mg C m^{-3})) for UK national marine areas, from the POLCOMS-ERSEM model (solid lines) and satellite observations (dashed line). The values have been smoothed with a 5-year kernel to show long-term trends. The anomaly is the difference from the mean value for 1998-2008.

Table 3.10 Temporal trend in surface log-chlorophyll concentration (log(mg C m^{-3}) per decade) for national regions and the UK EEZ, 1998-2021.

	UK EEZ	England	Wales	Scotland	N. Ireland
POLCOMS-ERSEM model	-0.038	-	-0.028	-0.059	-0.048
satellite obs	-	0.035	0.019	-0.026	0.008

The comparison to surface chlorophyll is an indirect measure of column total phytoplankton biomass, but it is likely to give a valid picture of spatial and temporal variation. Given the discrepancy in temporal trends, confidence is assessed as weak everywhere.

3.3.15 Bottom non-living organic carbon

There was insufficient observational evidence for an assessment to be made.

3.4 References for section 3

Barange, M., Merino, G., Blanchard, J.L., Scholtens, J., Harle, J., Allison, E.H., Allen, J.I., Holt, J., Jennings, S., 2014. Impacts of climate change on marine ecosystem production in societies dependent on fisheries. Nature Clim. Change 4, 211–216. https://doi.org/10.1038/nclimate2119

Bersch, M., Hinrichs, I., Gouretski, V., Sadikni, R., 2016. Hydrographic Climatology of the North Sea and Surrounding Regions (KNSC) version 2.0. Center for Earth System Research and Sustainability (CEN), University of Hamburg, Hamburg.

Blackford, J.C., Allen, J.I., Gilbert, F.J., 2004. Ecosystem dynamics at six contrasting sites: a generic modelling study. Journal of Marine Systems 52, 191–215. https://doi.org/10.1016/j.jmarsys.2004.02.004

Butenschön, M., Clark, J., Aldridge, J.N., Allen, J.I., Artioli, Y., Blackford, J., Bruggeman, J., Cazenave, P., Ciavatta, S., Kay, S., Lessin, G., van Leeuwen, S., van der Molen, J., de Mora, L., Polimene, L., Sailley, S., Stephens, N., Torres, R., 2016. ERSEM 15.06: a generic model for marine biogeochemistry and the ecosystem dynamics of the lower trophic levels. Geosci. Model Dev. 9, 1293–1339. https://doi.org/10.5194/gmd-9-1293-2016

Capuzzo, E., Lynam, C.P., Barry, J., Stephens, D., Forster, R.M., Greenwood, N., McQuatters-Gollop, A., Silva, T., van Leeuwen, S.M., Engelhard, G.H., 2018. A decline in primary production in the North Sea over 25 years, associated with reductions in zooplankton abundance and fish stock recruitment. Global Change Biology 24, e352–e364. https://doi.org/10.1111/gcb.13916

Donnelly, C., Andersson, J.C.M., Arheimer, B., 2016. Using flow signatures and catchment similarities to evaluate the E-HYPE multi-basin model across Europe. Hydrological Sciences Journal 61, 255–273. https://doi.org/10.1080/02626667.2015.1027710

Hall, A., Marsh, J., Clark, J., Kay, S., Fernandes, J.A., 2019. NEMO-ERSEM and POLCOMS-ERSEM: User Guides for Products (v1.1) (No. C3S_D422Lot2.PML.3.1_201907_Product_User_Guide_ERSEM_v1.1). ECMWF.

Hinrichs, I., Gouretski, V., Paetsch, J., Emeis, K., Stammer, D., 2017. North Sea Biogeochemical Climatology Technical Report. Hamburg.

Holt, J., Harle, J., Proctor, R., Michel, S., Ashworth, M., Batstone, C., Allen, I., Holmes, R., Smyth, T., Haines, K., Bretherton, D., Smith, G., 2009. Modelling the Global Coastal Ocean. Phil. Trans. R. Soc. A 367, 939–951. https://doi.org/10.1098/rsta.2008.0210

Holt, J.T., James, I.D., 2001. An s coordinate density evolving model of the northwest European continental shelf 1, Model description and density structure. J. Geophys. Res. 106, 14015–14,034. https://doi.org/10.1029/2000JC000304

Jolliff, J.K., Kindle, J.C., Shulman, I., Penta, B., Friedrichs, M.A.M., Helber, R., Arnone, R.A., 2009. Summary diagrams for coupled hydrodynamic-ecosystem model skill assessment. Journal of Marine Systems, Skill assessment for coupled biological/physical models of marine systems 76, 64–82. https://doi.org/10.1016/j.jmarsys.2008.05.014

Lauvset, S.K., Key, R.M., Olsen, A., van Heuven, S., Velo, A., Lin, X., Schirnick, C., Kozyr, A., Tanhua, T., Hoppema, M., Jutterström, S., Steinfeldt, R., Jeansson, E., Ishii, M., Perez, F.F., Suzuki, T., Watelet, S., 2016. A new global interior ocean mapped climatology: the 1° × 1° GLODAP version 2. Earth System Science Data 8, 325–340. https://doi.org/10.5194/essd-8-325-2016

Meinshausen, M., Smith, S.J., Calvin, K., Daniel, J.S., Kainuma, M.L.T., Lamarque, J.-F., Matsumoto, K., Montzka, S.A., Raper, S.C.B., Riahi, K., Thomson, A., Velders, G.J.M., van Vuuren, D.P.P.,

2011. The RCP greenhouse gas concentrations and their extensions from 1765 to 2300. Climatic Change 109, 213. https://doi.org/10.1007/s10584-011-0156-z

Miller, P.I. (2009) Composite front maps for improved visibility of dynamic sea-surface features on cloudy SeaWiFS and AVHRR data. Journal of Marine Systems, 78(3), 327-336, doi: 10.1016/j.jmarsys.2008.11.019

OSPAR (2017). Marine Climate: Prevailing Conditions and Climate Change. Intermediate Assessment 2017. Available at: https://oap.ospar.org/en/ospar-assessments/intermediate-assessment-2017/climate-and-ocean-acidification/marine-climate-prevailing-conditions-and-climate-change/

Ostle C., P. Williamson, Y. Artioli, D. C. E. Bakker, S. Birchenough, C. E. Davis, S. Dye, M. Edwards, H. S. Findlay, N. Greenwood, S. Hartman, M. P. Humphreys, T. Jickells, M. Johnson, P. Landschützer, R. Parker, D. Pearce, J. Pinnegar, C. Robinson, U. Schuster, B. Silburn, R. Thomas, S. Wakelin, P. Walsham, and A. J. Watson (2016) Carbon dioxide and ocean acidification observations in UK waters: Synthesis report with a focus on 2010-2015, doi: 10.13140/RG.2.1.4819.4164

Taylor, K.E., Stouffer, R.J., Meehl, G.A., 2011. An Overview of CMIP5 and the Experiment Design. Bull. Amer. Meteor. Soc. 93, 485–498. https://doi.org/10.1175/BAMS-D-11-00094.1

3.5 Acknowledgements for section 3

This study has been conducted using E.U. Copernicus Marine Service Information: https://doi.org/10.48670/moi-00169, https://doi.org/10.48670/moi-00281, https://doi.org/10.48670/moi-00283, https://doi.org/10.48670/moi-00047.

4 Environmental variables in the sea bed (ERSEM benthic)

This section gives validation information about the benthic variables used in the conservation meta-analysis: sediment organic carbon and the oxygen penetration depth. POLCOMS-ERSEM model outputs were compared to observation-based statistical models.

4.1 Model description

As well as the pelagic model described in section 3, ERSEM, the European Regional Seas Ecosystem Model, has a separate benthic model (Butenschön et al., 2016). This is fully coupled to the pelagic component and handles transfers of carbon and nutrients at the sea bed and within sediment (see Figure 3.1). The benthic model has aerobic and anaerobic bacteria and three feeding groups: filter feeders, suspension feeders and meiobenthos. The last of these contribute to mixing through the sediment by bioturbation. Oxygen levels in the sediment gradually decrease away from the water surface and the oxygen penetration depth is a model output. Sediment organic carbon is separated into dissolved organic matter and degradable, refractory and buried particulate carbon; in model nomenclature the particulate types are called Q6c, Q7c and Q17c respectively. Any carbon that reaches the bottom layer cannot be returned to the water column and becomes buried carbon; it should be noted that this is not calibrated to represent stocks of buried carbon in real-world conditions.

4.2 Validation methodology

4.2.1 Sediment organic carbon

Diesing et al., (2017; 2021) describe a method of estimating sediment particulate organic carbon (POC) density (g m^{-3}) with only sparse observations using a quantile regression forest (QRF)

algorithm applied to a set of predictor variables (Table 1). The resulting maps of predicted carbon content in the top 10cm of the bed (Diesing et al., 2017) were compared visually with contour maps of total organic carbon from ERSEM. In addition, the underlying carbon data, along with additional data from the Agri-Food and Biosciences Institute (AFBI), was compared with the co-located ERSEM model predictions(Figure 1A). The data points used to derive the original statistical map are shown in Figure 1B.

Table 4.1 Predictor variables used for benthic organic carbon prediction ranked in order of importance (see Diesing et al., 2017, for details).

1.	% Mud content
2.	Average bottom temperature
3.	Distance to shoreline
4.	Eastings
5.	%Gravel content
6.	Peak wave orbital velocity

POLCOMS-ERSEM total sediment POC content (g C m^{-2}) was calculated as the sum of slowly degradable carbon (ERSEM variable Q6c) and available refractory carbon (ERSEM variable Q7c) by taking the mean of monthly mean values for the period 2006-2009. Examination of the e-folding depths associated with the modelled exponential profiles for Q6c and Q7c were less than 4cm everywhere indicating that much of the model POC can be considered to be contained within the top 5cm of the bed and can be reasonably compared with the observed 5cm carbon stock values. The modelled buried refractory carbon (ERSEM nomenclature Q17c) was considered separately in the comparison as nominally it represents carbon below the ERSEM total sediment depth of 30cm. The overall conclusions are not affected by the inclusion of this pool.

The AFBI data consists of benthic organic carbon measurements in the top 5cm of the bed at near annual frequency starting from 1999 and continuing to the present time at 6 locations off the Northern Irish coast (Figure 4.2A). The observations show large variability between samples with some suggestion of a trend to higher carbon content over time (Figure 4.2B). Original data was expressed as the carbon weight to weight of inorganic sediment. Contemporaneous measurements of porosity were not available. For comparison with the ERSEM model a crude conversion to g C m^{-2} (5cm) was carried out using measured average sediment water content (by weight) and assumed water and sediment densities of 1025 and 2650 kg m^{-3}, respectively. Because of high the sample variability, data were not averaged, and all samples were included in the scatter plot (Figure 4.3).

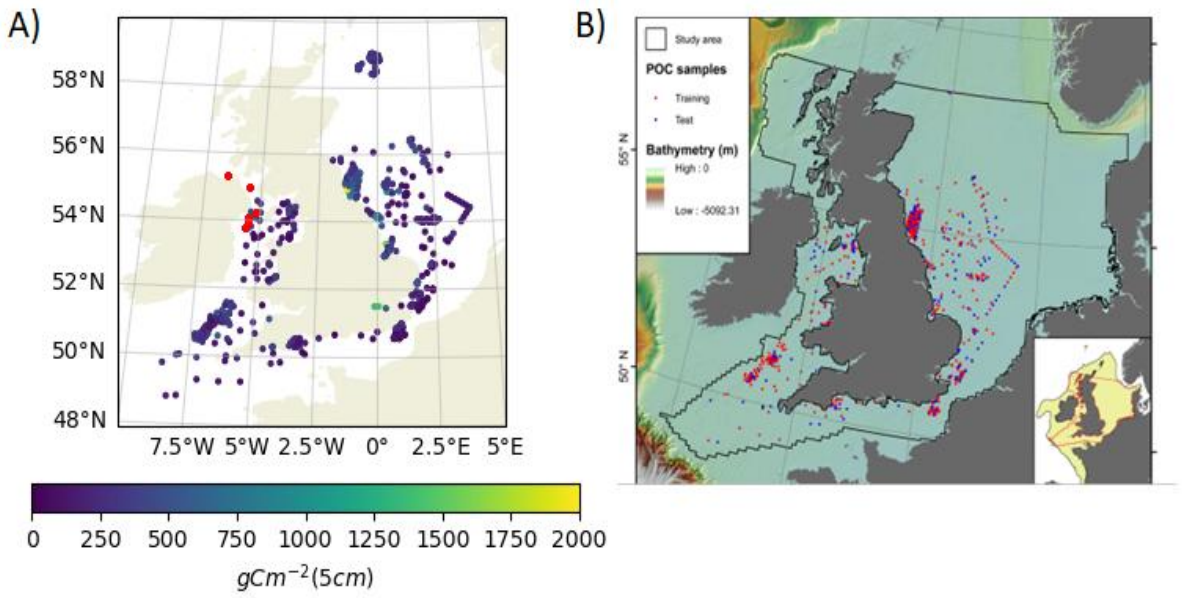

Figure 4.1. Sediment organic carbon observations: A) Diesing et al. (2017) and AFBI data (red dots) used to compare directly with ERSEM (Figure 4.2). B) Diesing et al. (2017) used to derive spatial map (Figures 4.3A)

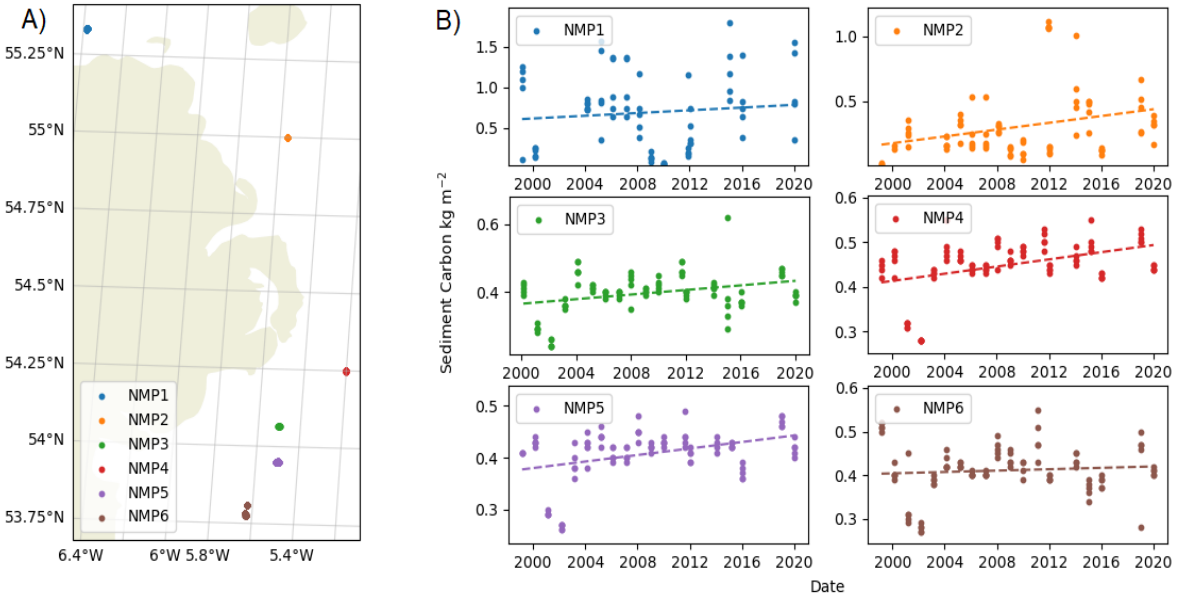

Figure 4.2: A) Locations for AFBI data. B) Time series plots of 5cm stocks.

4.2.2 Depth of the oxygen horizon (oxygen penetration depth)

The depth of the oxic layer in the seabed (oxygen penetration depth, OPD, ERSEM name “depth of oxygen horizon”) is often considered the region where breakdown of organic matter occurs most

rapidly. OPD depends on both the rate at which dissolved oxygen exchanges with the water column and the benthic oxygen consumption. A larger (deeper) OPD value generally indicating less benthic oxygen demand and/or faster exchange with the overlying oxygenated water. Observations suggest a sharp transition from deeper to shallow OPD once the percentage fine content (mud + silt) exceeds around 10% (Parker et al., 2012; 2011). This is attributed to a change from advective pore water driven transport behaviour to diffusive transport controlled by the sediment permeability.

In Parker et al. 2011; 2012, a simple form of parametric bootstrapping (Manly, 1998) was used to derive a 'broken stick' profile to predict model oxygen penetration depths (OPD) based on the %silt content of sediments.

$$OPD = \exp(1.250 - 0.014SILT) \qquad \text{for \%silt} \leq 10.1$$

$$OPD = \exp(-0.0187) \qquad \text{for \%silt} > 10.1$$

Combining this with the maps of the observed distribution of seabed silt content allowed a tentative spatial map of OPD to be derived.

4.3 Validation outcomes

4.3.1 Sediment organic carbon

A scatter plot of observed sediment organic carbon content (Figure 4.3) against POLCOMS-ERSEM results (Q6c + Q7c) at the same locations showed model values typically a factor of 10 to 30 less than observed values (10-20 less if Q17c is included). No discernible trend or correlation is apparent between observed and modelled values nor with respect to distance from shore.

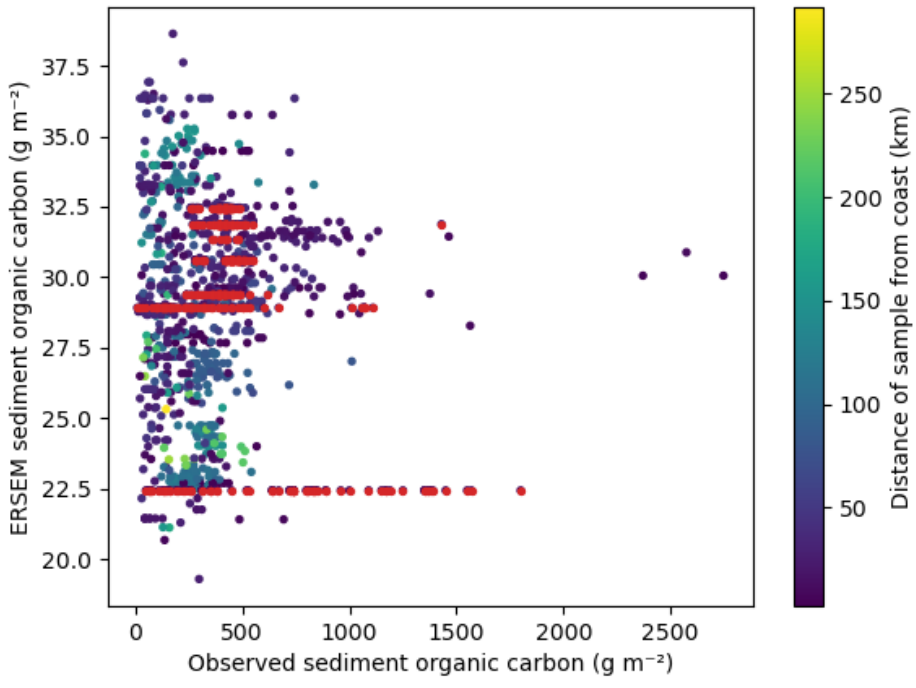

Figure 4.3. benthic organic carbon content in top 5cm (g m^{-2}) scatter plot. X-axis observations used by Diesing et al. 2017 (see Figure 1A) and also AFBI data (marked red) . Y-axis are POLCOMS-ERSEM 2006-2009 mean at matched locations. Marker colour is scaled to the distance from the coast, as a possible explanatory variable, apart from AFBI data shown in red.

The disparity between modelled and measured benthic POC stocks has been noted previously (e.g. Aldridge et al., 2017). This is interpreted to be a consequence of the different particulate carbon fractions present in the seabed. Marine biogeochemical models such as ERSEM deal primarily with the relatively labile organic material remineralised over timescales of months, that are responsible for much of the short-term features of the benthic carbon cycle, including observed benthic CO_2 fluxes and faunal biomass. The large pool of benthic carbon unaccounted for by the model is, by contrast, likely to be relatively refractory and less important for biological processes, although it may be important in terms of carbon sequestration.

Spatial patterns of modelled benthic carbon stock were compared with the data derived statistical maps. Given the large difference in magnitude indicated in Figure 4.3, both data driven and modelled distributions were normalised to lie in the interval [0, 1] to more clearly show relative spatial patterns. Since both data sets contain some outliers, the 10th to 90th percentile was used to define the upper and lower bounds in the normalisation. The resulting maps of sediment POC content for the data driven maps (Figure 4.4, A) and POLCOMS-ERSEM (Figure 4.4, B) show markedly different patterns. The data driven approach shows the strongest correlation with sediment type (especially mud content) followed by bottom temperature (Diesing et al., 2017; see also Wilson et al., 2018). This gives, for example, relatively higher predicted organic carbon content in the cooler, muddier northern North Sea sediments (Figure 4.2B) and at known localised mud patches in the Irish and Celtic seas. By contrast, the ERSEM model showed largest seabed organic carbon content in coastal zones and the southern North sea and correlated to modelled water column productivity. This is consistent with the hypothesis that measured and the modelled carbon are representing different carbon pools.

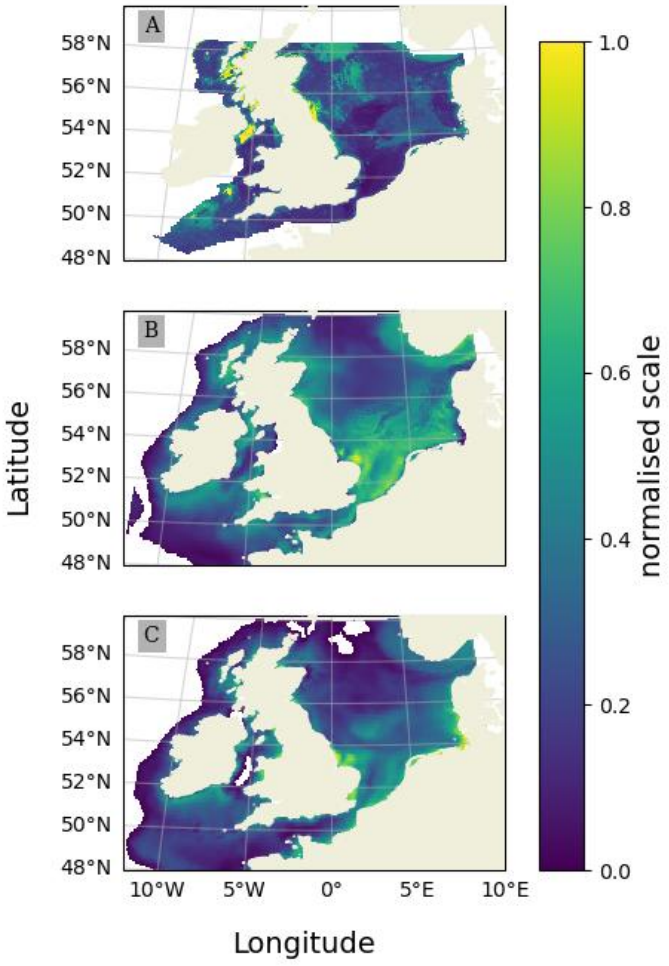

Figure 4.4. Normalised benthic organic carbon. A) data driven map (Diesing et al (2017), B) POLCOMS-ERSEM model, 2006 to 2009 mean, C) chlorophyll-a concentration, 2006 to 2009 mean averaged over the euphotic depth.

In summary, we conclude that the available observational cannot be directly compared to the ERSEM-derived dataset. In addition, there is insufficient observational data to assess change over time. We conclude that there is not enough evidence to assign a confidence level, although the analysis presented here provides some information about where the model outputs may be more or less reliable.

4.3.2 Depth of the oxygen horizon (oxygen penetration depth)

The statistical correlation based map of OPD was compared (Figure 4.5) to the POLCOMS-ERSEM model data for oxygen horizon depth (ERSEM variable D1M). In general, model values show a shallower depth compared to the data derived distribution. To bring out spatial patterns, the values were normalised to the interval [0,1] based on 10^{th} and 90^{th} percentiles. The data driven distribution is determined by the %fines content, with a transition from shallow to deeper oxic layers when fine content < ~10%, so it essentially picks out the difference between muddy and sandy/gravely sediments, with thinner oxic zones muddy regions. This gives a different distribution compared to the ERSEM-derived dataset (Figure 4.6). Sediment type is not strongly distinguished in the ERSEM model and OPD here appears to be partly linked to water depth (see depth contour in Figure 4.6 B). For the model, it is hypothesised that the deeper oxic layer in the northern North Sea is due to less organic material reaching the bed in deeper water (possibly in conjunction with decreased microbial oxygen consumption with lower temperatures) leading to reduced benthic productivity and consequent oxygen demand.

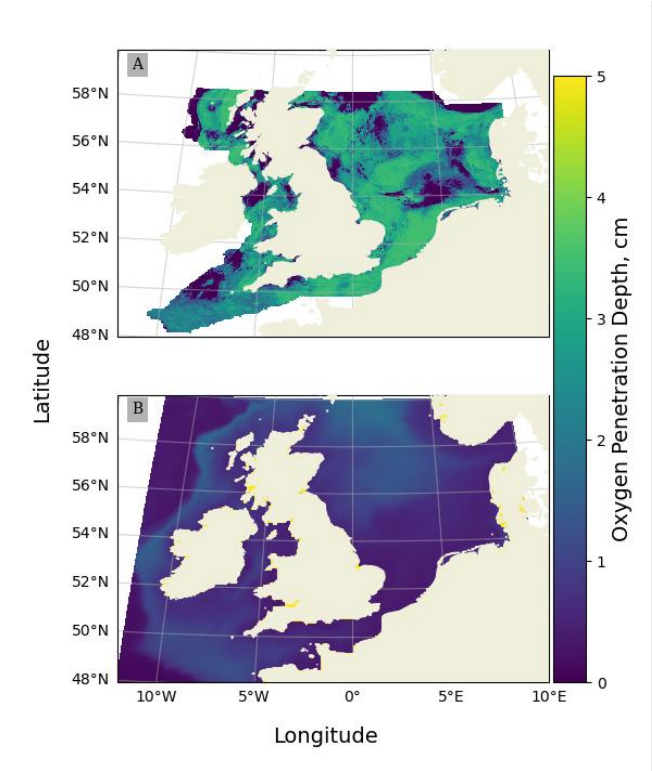

Figure 4.5. Oxygen penetration depth (cm) maps from, A) statistical correlation based on %silt content, B) POLCOMS-ERSEM model.

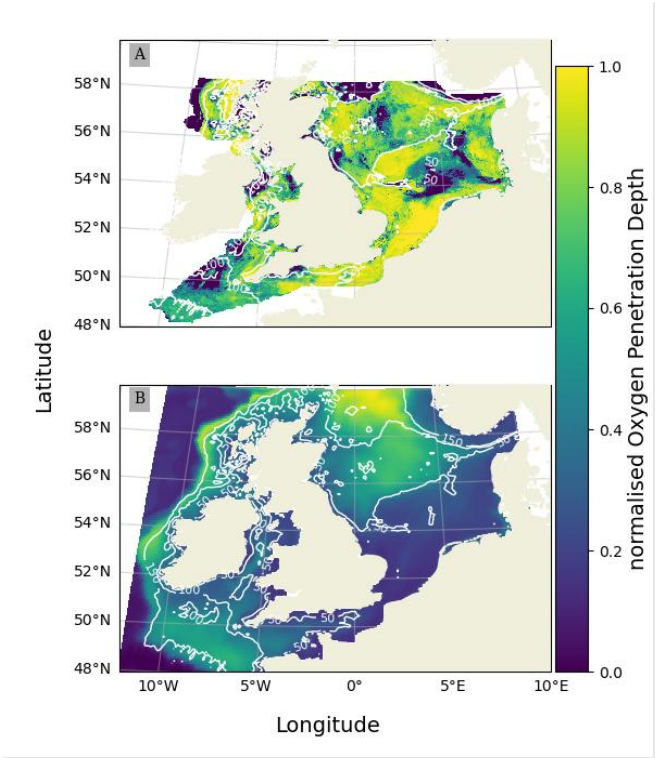

Figure 4.6. Normalised oxygen penetration depth maps from, A) statistical correlation based on sediment size, B) POLCOMS-ERSEM model. White lines are contours of 50m, 100m and 150m water depth.

In summary, the ERSEM model lacks the distinction between muddy and sandy sediment processes, linked to permeability, that should enable better prediction of the oxygen penetration depth. The spatial variability derived from correlating observations with %fine content is not reflected by the model dataset and we therefore assign weak confidence to this variable. There is insufficient data to assess trends over time.

4.4 References for section 4

Aldridge, J., Lessin, G., Amoudry, L.O., Hicks, N., Hull, T., Klar, J.K., Kitidis, V., McNeill, C.L., Ingels, J., Parker, E.R., Silburn, B., Silva, T., Sivyer, D.B., Smith, H.E.K., Widdicombe, S., Woodward, E.M.S., van der Molen, J., Garcia, L., Kröger, S., 2017. Comparing benthic biogeochemistry at a sandy and a muddy site in the Celtic Sea using a model and observations. Biogeochemistry 135, 155–182. doi:10.1007/s10533-017-0367-0

Butenschön, M., Clark, J., Aldridge, J.N., Allen, J.I., Artioli, Y., Blackford, J., Bruggeman, J., Cazenave, P., Ciavatta, S., Kay, S., Lessin, G., van Leeuwen, S., van der Molen, J., de Mora, L., Polimene, L., Sailley, S., Stephens, N., Torres, R., 2016. ERSEM 15.06: a generic model for marine biogeochemistry and the ecosystem dynamics of the lower trophic levels. Geosci. Model Dev. 9, 1293–1339. https://doi.org/10.5194/gmd-9-1293-2016

Diesing, M., Kröger, S., Parker, R., Jenkins, C., Mason, C., Weston, K., 2017. Predicting the standing stock of organic carbon in surface sediments of the North–West European continental shelf. Biogeochemistry 135, 183–200. doi:10.1007/s10533-017-0310-4

Diesing, M., Thorsnes, T., Bjarnadóttir, L.R., 2021. Organic carbon densities and accumulation rates in surface sediments of the North Sea and Skagerrak. Biogeosciences 18, 2139–2160. doi:10.5194/bg-18-2139-2021

Manly, B. F. J., (1998). Randomization, bootstrap and monte carlo methods in biology: 2nd Edition. Chapman and Hall, London.

Parker, R., Lees, H. and J. Barry (2011). Summary report on variability in oxygen penetration within and among the Ecohydrodynamic Units (EHUs) identified for the North Sea. Contract report ME5301

Parker, R., Weston, K., Barry, J. and C. Powell (2012). Recommended biogeochemical targets and indicators for MSFD monitoring and management of the UK seabed. Contract report ME5301.

Wilson, R.J., Speirs, D.C., Sabatino, A., Heath, M.R., 2018. A synthetic map of the north-west European Shelf sedimentary environment for applications in marine science. Earth Syst. Sci. Data 10, 109–130. doi:10.5194/essd-10-109-2018

5 Fish species (SS-DBEM model)

Author: Sevrine Sailley, sesa@pml.ac.uk

5.1 Model description

5.1.1 SS-DBEM in a nutshell

The Size Spectra – Dynamic Bioclimate Envelope Model (SS-DBEM) is a state-of-the-art model that projects the impact of changes in the environment and human activity on the abundance, biomass, and distribution of modelled species, whilst considering their ecology and physiology. Therefore, the SS-DBEM can project fish distribution and trends in response to climate change. It is important to note that the model is the full species distribution not specific stocks. The model does not try to simulate the exact number of individuals of a given species, but rather the relative number of individuals compared to other areas and other times. As such, while model units are expressed as "Number of individuals", they are not to be used to predict future stock; rather, trends in response to changes in climate and fishing management.

SS-DBEM use the following environmental conditions data from climate model projections:

- Primary production
- Bottom temperature
- Surface temperature
- Sea water pH
- Sea water Salinity
- Oxygen concentration
- Ocean currents

These are necessary to account for habitat suitability (e.g. temperature, salinity and pH), defining the size spectrum and system carrying capacity (i.e. chlorophyll), dispersion (current), and impacts on metabolic rate (e.g. temperature).

5.1.2 Model initialisation

The outputs from climate models are used to drive the SS-DBEM, which projects changes in fish species distribution and biomass while explicitly considering known mechanisms of population dynamics and dispersal (both larval and adult), as well as eco-physiological changes caused by changing ocean conditions (Cheung et al., 2011; Fernandes et al., 2013; Fernandes et al., 2020). The SS-DBEM is a combined mechanistic-statistical approach that has been applied to a large number of marine species globally and is one of the models participating in the Fisheries model inter-comparison program (FISHMIP; Tittensor et al., 2018; Lotze et al., 2019).

Initial distributions of selected species in the SS-DBEM are first estimated using the Sea Around Us database method (Close et al., 2006). Using data primarily derived from FishBase (www.fishbase.org) and SeaLifeBase (www.seaaroundus.org), it determines distribution based on (see Close et al., 2006 for more details on the method):

a) presence
b) latitudinal range
c) range limiting polygons
d) depth range
e) habitat preference
f) the effect of "equatorial submergence"

Then, the suitability of each species to different environmental conditions (e.g. temperature, salinity, oxygen concentration, bathymetry) is defined using its model-inferred environmental preference profile (see Cheung et al., 2008a; 2009 for more details), which create seed populations. The model is initialized with these seed populations using the estimated present distribution and then driven by ocean model outputs to evaluate the impact of recent (Queirós et al., 2018) or future (Fernandes et al., 2016) changes in environmental conditions on fish populations distribution. Combining ocean dynamics (e.g. advection) with mortality, growth, and dispersal processes, the model projects future patterns in distribution and biomass (see Cheung et al., 2008, 2009, for more details) with the carrying capacity of each species being dependent on the environmental conditions and limited by primary production. The Size Spectra component of the SS-DBEM accounts for resource by comparing the biomass that can be supported in any given area (based on primary production and the derived size spectrum) to the energy demand of the species that are predicted to be present in the area. Energy is distributed to species in proportion to their energy demand and their growth rate (see Fernandes et al., 2013 for details). Because the model accounts for both environmental preference and population dynamics, any changes in environmental conditions will result in changes in life history (e.g. growth, migration), carrying capacity, and, consequently on the abundance and distribution of species.

The SS-DBEM fisheries model was initiated with seed populations for each species in 1990 and run until 2099. As mentioned, the model calculated biomass of fish each year after migration, reproduction and death (both natural and through fishing) were taken into account. Trial experiments in our study showed that the model reaches a stable state in under 10 years when run with constant conditions. We therefore treated the first 10 years of a model run as spin-up and only report changes between 2000 and 2099. The model was run on a global configuration, where all of the world's oceans are represented, to overcome any boundary condition issues. It is worth noting that the model is capable to run 100s of species globally (see Cheung et al., 2019) and as such does not need specific parameterization for this regional application with the species selected and the forcing being the only change.

5.1.3 Assumptions of the model

The Dynamic Bioclimate Envelop Model modelling approach has a number of inherent assumptions and uncertainties that may affect the performance of the model (RD.3). Firstly, the model is based on the assumption that the current predicted species distributions depict the environmental preferences of the species and are in equilibrium. Secondly, the underlying biological hypothesis, represented by the model structure and input parameters, may be uncertain. Moreover, the models did not consider the potential for phenotypic and evolutionary adaptations of the species.

Theoretical and empirical data were used to model trophic interactions. The modelling approach does not incorporate the full range or complexity of interactions among species, but avoids the difficulties of formalising transient and complex species-specific predatory interactions at large-scales. It also requires no assumptions about the extent to which species-specific trophic interactions that are currently observed will persist in the future. Furthermore, at the system level, size-based processes account for much of the variation in prey choice and trophic structure.

5.1.4 Limitations of the model outputs

5.1.4.1 Data used to drive the model

The simulations used in MSPACE were run using inputs from three marine hydrodynamic-biogeochemical models: the POLCOM-ERSEM, NEMO-ERSEM and GFDL models.

The POLCOMS-ERSEM, NEMO-ERSEM, and GFDL models were driven by one Coupled Model Inter-comparison Project Phase 5 (CMIP5) global climate model (GCM) projections with downscaled atmospheric data from a regional climate model (RCM), the Swedish Meteorological and Hydrological Institute (SMHI) Rossby Centre Regional Atmospheric Model (RCA4). Using only one of the many possible combinations of GCM-RCM pairs leads to an incomplete estimate of the true uncertainty in the outcome in a changing climate by, most likely, indicating a smaller spread of outcomes than if the estimate were based on a larger ensemble of such GCM-RCM combinations. This does not necessarily mean a reduction in the true uncertainty, but simply an incomplete estimate of it. See section 3.2.4 for more information on the data used to drive the model.

POLCOMS-ERSEM and NEMO-ERSEM have a different model for the physics (POLCOMS and NEMO), but the same model for the biology and biogeochemistry (ERSEM). So while some different behaviour is expected in the physics the response of the primary production to it will be the same so there are similarities between those two. The GFDL model is entirely different and is expected to stand out from the rest. This means that in case where we have projections for the GFDL and one or both of the ERSEM there will be a divergence between them.

5.1.4.2 Interpretation of model outputs

Whilst the model units are expressed as “Number of individuals”, they are not to be used to predict actual future stocks but rather numbers relative to the initial starting values of the model. This is because the model was not initialised with actual fish numbers and subsequently the significance of this dataset is to show temporal and geographical trends, relative to other years and other grid points, in response to changes in the climate and the applied Maximum Sustainable Yield (MSY). Another limitation comes from the MSY itself, the amount of pressure and fishing will vary according to the abundance of the individual fish species but the MSY will be constant, meaning that fishing will happen as long as there is fish to be fished in the model. Also, the same MSY is applied to all species which is not realistic when it comes to management of the fisheries since the quota and ensuing fish pressure are re-evaluated on a regular basis. But it does provide an opportunity to see

what the impact of fishing is on top of that of the climate change. Consequently, we are only looking for trends in abundance and changes in distribution rather than absolute values of fish whether it be in the present (validation period) or the future.

5.2 SS-DBEM methodology

5.2.1 Target species

Species of fish used in validation were selected on the following basis:

1. Availability of pre-existing model output for this species
2. Species is present in UK waters and contribute a significant
3. Used in the Marine Spatial planning analysis

Consequently, we carried on the exercise for the species listed in Table 5.1, note that some of the species were present in all models and others were only in one. The goal is not to compare the SS-DBEM response to the different biogeochemical model used to provide the environmental data but whether it matters and the impact it can heave on the confidence in the model output for the larger analysis.

Table 5.1: list of Species that were validated and model that provided the output

Fish species	POLCOMS ERSEM	NEMO ERSEM	GFDL	ERSEM
Clupea harengus	x	x	X	
Merluccius merluccius	x	X		
Micromesistius poutassou	x	x	X	
Dicentrarchus labrax	x	X		
Gadus morhua	x	x	X	
Scomber scombrus	x	x	X	
Salmo salar	x	X		
Malotus villesus			X	
Solea solea	x	x	X	
Pleuronectes platessus	x	x	x	
Pollachius virens	x	x	X	
Scophthalmus maximus	x	X		
Sardina pilchardus	x	X		
Sprattus sprattus	x	x	X	
Trachurus trachurus	x	x	X	
Hipoglossus hipoglossus	x	X		
Melanogrammus aeglefinus			X	

Nephrops norvegicus				x

5.2.2 Scenarios

When talking of scenario for the model we consider two things: i) the climate forcing (that is the Representative Concentration Pathway, RCP) that is being implemented in the biogeochemical model; and ii), the fishing intensity applied in the SS-DBEM as represented by the MSY.

Fishing scenarios are defined relative to each species' maximum sustainable yield (MSY). Here, MSY is the highest average theoretical equilibrium catch that can be taken continuously from a stock under average environmental conditions (Hilborn and Walters, 1992). Assuming a simple logistic population growth function and under equilibrium conditions, MSY is calculated as:

MSY = (B*intR)/4

where intR is the intrinsic rate of population increase and B is the biomass at a species' carrying capacity (Schaefer, 1954; Sparre and Venema, 1998). In this model, the intR for each species is calculated based on natural mortality (Pauly, 1980; Cheung et al., 2008b). Note that MSY is linked to the fishing mortality rather than the biomass.

The combination of RCP and MSY created a number of scenarios (table 5.2) that are similar to Shared socio economic scenarios and provide information on both the impact of climate change and that of human activity (fisheries).

Table 5.2: Model scenario in MSPACE

Model	RCP	MSY
POLCOMS-ERSEM	4.5	0, 0.6
	8.5	0, 0.8, 1.1
NEMO-ERSEM	4.5	0.6
	8.5	0.8, 1.1
GFDL	2.6	0
	8.5	0
ERSEM	2.6	0
	8.5	0

5.2.3 Model spatial and temporal scale

The model outputs are on a 0.5 by 0.5 degree grid meaning it is composed of squares that are roughly 50 by 50 kilometres. The spatial domain covered by the SS-DBEM outputs is determined by the spatial domain of the biogeochemical model used to provide the environmental variables, since they all cover the full UK waters, this is not an area of concern. The model outputs are expressed as an annual value that represent the potential abundance of fish within each grid square of the model

A previous validation exercise (Fernandes et al., 2020) showed that the model could reproduce trends in survey data for the period 1970-2000. For the biogeochemical models that provide the environmental variables to the SS-DBEM this correspond to the historical period, that is the atmospheric forcing is provided by data rather than by atmospheric model. Here we will focus on the years 2000 to 2020, this means that atmospheric forcings for this time period are provided by atmospheric model and while there will be little variation between different climate scenario, some divergence might happen.

5.3 Validation methodology

5.3.1 Model and survey data availability

- Survey data: Lynam et al, Cefas (2022). A data product derived from Northeast Atlantic groundfish data from scientific trawl surveys 1983-2020. Cefas, UK. V1. doi: https://doi.org/10.14466/CefasDataHub.126
- SS-DBEM projections using POLCOMS-ERSEM and NEMO-ERSEM model outputs: Sailley, S., Kay, S., Clark, J.R., Calton, B., (2020): Fish abundance and catch data for the Northwest European Shelf and Mediterranean Sea from 2006 to 2098 derived from climate projections. Copernicus Climate Change Service (C3S) Climate Data Store (CDS). 10.24381/cds.39c97304
- SS-DBEM projections using GFDL model outputs (Fernandes et al., 2013, 2020)

5.3.2 Data handling

Survey data location was matched to the SS-DBEM grid by using a nearest neighbour approach to ensure geographical match when selecting a specific domain for the analysis. Domains of choice were the UK EEZ and each national marine plan areas (Figure 3.3). The data were aggregated over the whole areas, with no distinction between inshore and offshore areas as the model resolution did not allow for this.

From there, survey data and model output were filtered for a specific area and aggregated temporally or spatially depending on the end goal of that validation. Next, data were normalised so they vary between 0 and 1. This is done to ensure we compare variability and trends which are the important information in the analysis rather than actual number of fish in either survey or model.

Once normalised the model outputs are compared to each other in a number of way:

1. Temporal match:
    a. Trend: do the trend in model outputs match those in the survey on a year to year basis
    b. Difference: what is the difference between survey and model output? Does the model overestimate or underestimate on an annual basis?
    c. Mean difference: the mean value of the difference to estimate how much the model divert from the data on a decadal basis.
2. Spatial match: does the model capture the spatial variability inherent in the marine ecosystem.
3. Do scenario matter? Throughout we're comparing different scenario as well as different forcing model used to provide the environmental data needed by the model. This will inform how much is behaviour inherent to the model and how much indicate response to the forcing.

Note that for a few species we had enough data to generate a trend at the UK EEZ scale but not at the National Marine Plan scale, while there might be survey data if not enough sites are repeated every year or are just one offs. Causing data sparsity once we move to a smaller spatial domain.

Spatial distribution could still be plotted in these cases, as we average over time, though it also shows that in same case the highest survey density is outside of the UK EEZ.

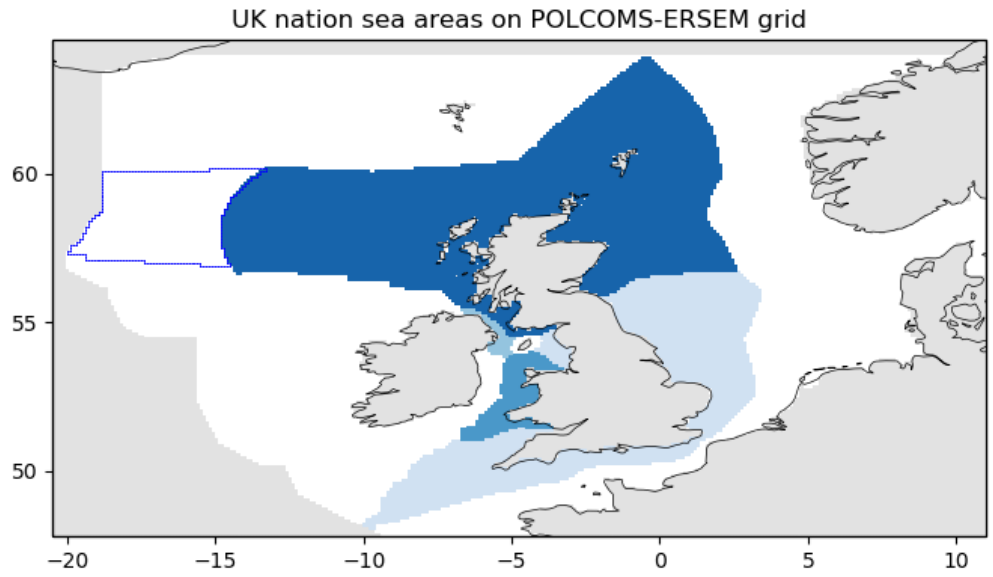

Figure 5.1: Map of the 4 National marine plan area (placeholder figure)

5.4 Validation outcome

5.4.1 Temporal scale

5.4.1.1 Trends

Overall, we found good agreement between the model scenarios (Figures 5.2-5.6). This means that for the present time period, when the climate signal is weak, there is little impact of the scenario used. Divergence are due to the different fishing pressure applied or the use of a significantly different biogeochemical model to provide the environmental variables. There appear to be little agreement between the survey data and the model trends, though for the second half of the time period considered there seems to be more agreement between the model and observations. It is important to note that the survey data were not filtered for specific survey quarters or size of individual, the model is likely better equipped to capture trends in larger adult individual than the juveniles or smaller individuals, plus it provides a value for the year as a whole rather than a specific timing that can be match with survey timing. So some mismatch between survey data and model output are to be expected.

For most fish species it looks like the trend is slightly off for the first few years, which could be due to the model coming out of what is known as the spin-up period (1980-2000). That is the model was still being initialised and the projected trend might be a bit off. For the second half of the period, we see that trends start to match, though with a delay of a few years. There is a spread within the models trends in response to both the model used to provide environmental variables and the scenarios used (climate and fishing combination). Overall, there is minimum spread between the model reflecting that the climate scenarios have not yet heavily diverged and small effects of either climate or fishing pressure are driving the variations.

UK EEZ	England	Scotland	Wales	N. Ireland
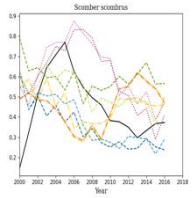	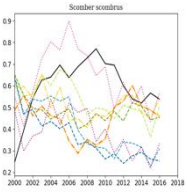	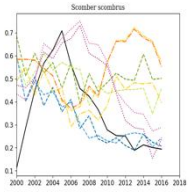	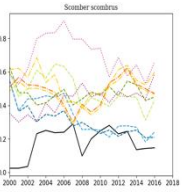	Not enough data
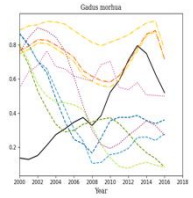	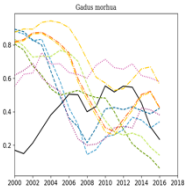	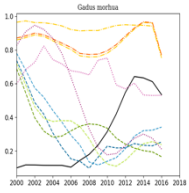	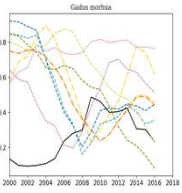	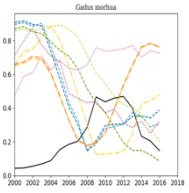
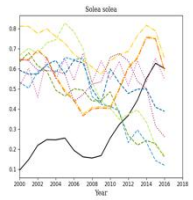	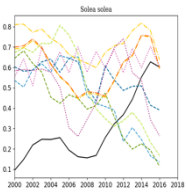	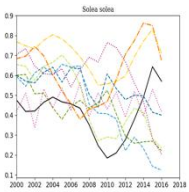	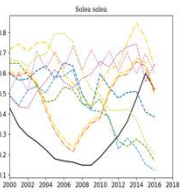	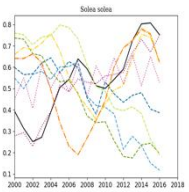
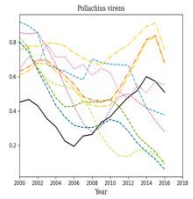	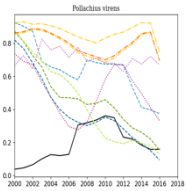	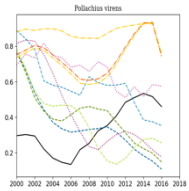	Not enough data	Not enough data
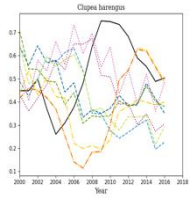	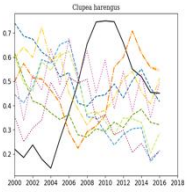	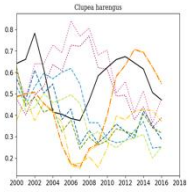	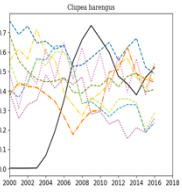	
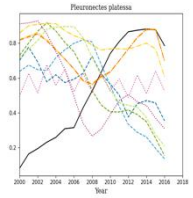	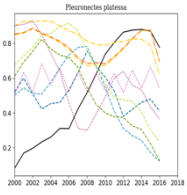	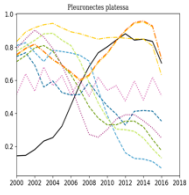	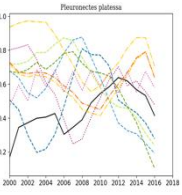	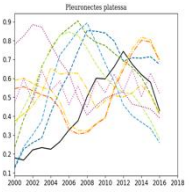
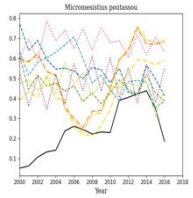	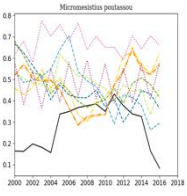	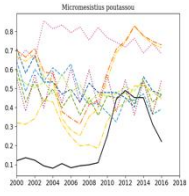	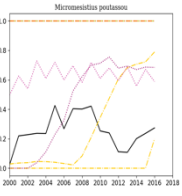	Not enough data
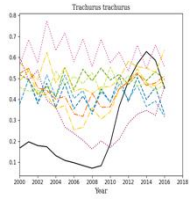	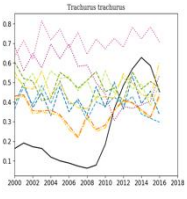	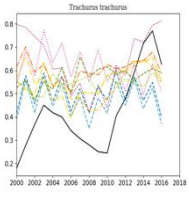	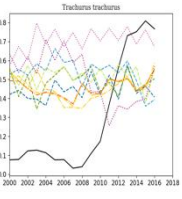	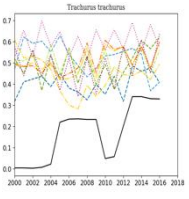

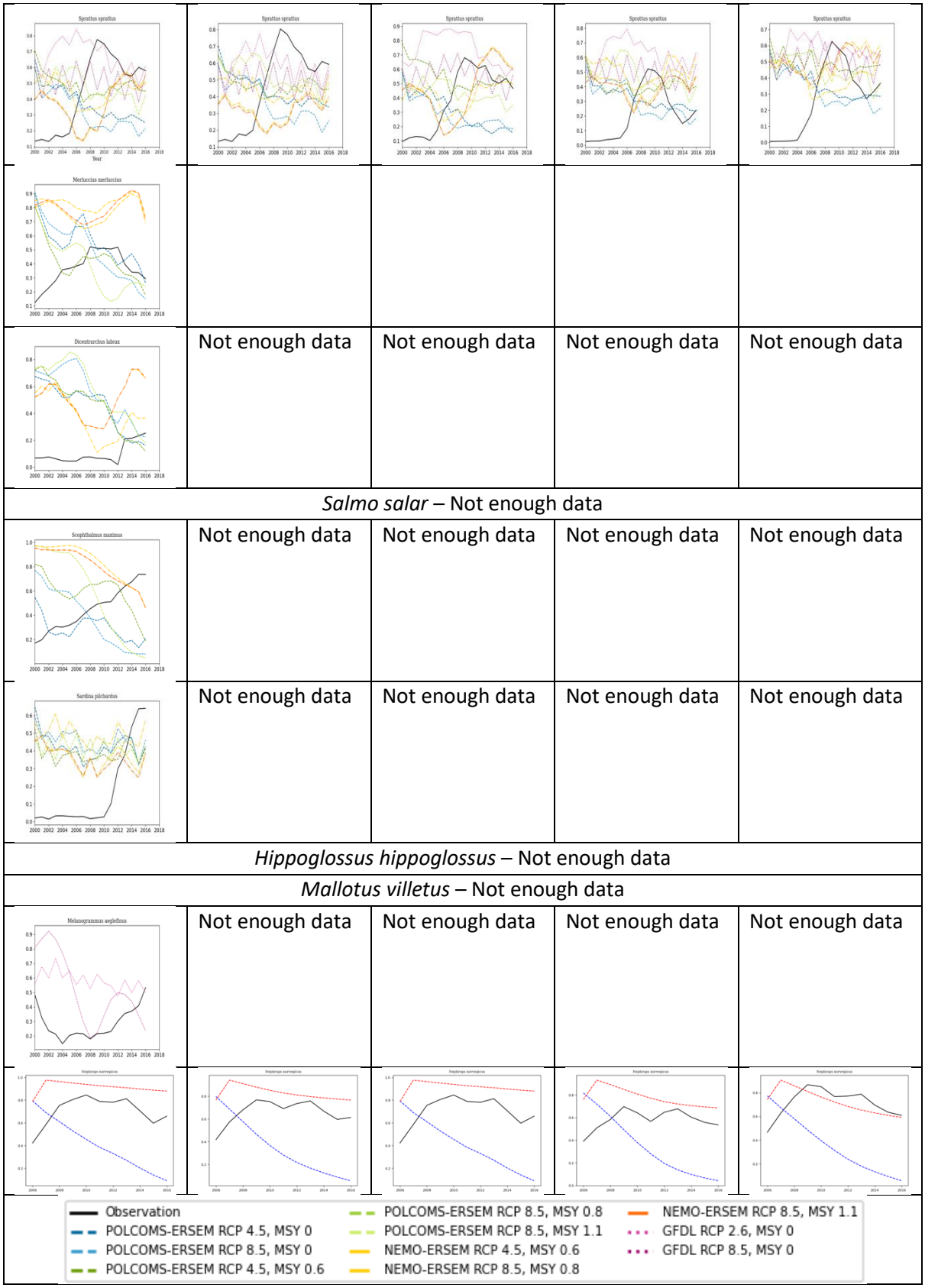

Figure 5.2: Temporal trends at the UK EEZ scale. Black line reflects the trend in the observations while the various colours correspond to the biogeochemical model used and the various scenarios. The red and blue lines for Nephrops norvegicus represent the RCP8.5 (red) and RCP 2.6 (blue).

5.4.1.2 Model to survey data temporal trend difference

Subtracting the data from the model shows us how far the model is from the observation as well as whether it tends to overestimate or underestimate the trend (Figures 5.7-5.11). Optimally we'd want all results from this to be as close to zero as possible. The difference in trend confirms what we found earlier in that in the early 2000s all models are overestimating the biomass compared to the survey data on a year-to-year basis. This overestimate gets reduced for most species, though in some cases it becomes an apparent underestimate this is likely from the delay between model and data that we mentioned earlier.

Except for some instances, all models are quite close to each other with the error and the range is within +/-0.5 indicating that the difference between model and data is not overwhelming.

UK EEZ	England	Scotland	Wales	N. Ireland
		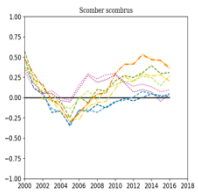		Not enough data
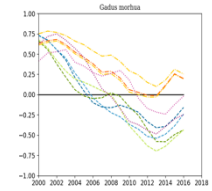	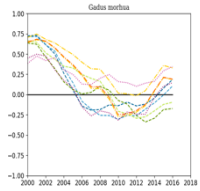	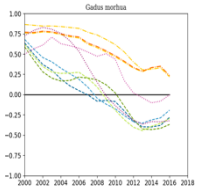	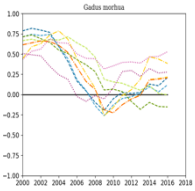	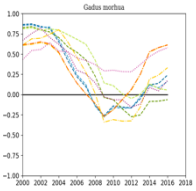
			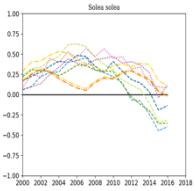	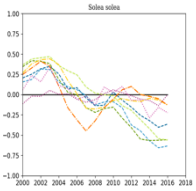
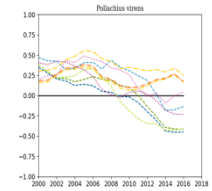	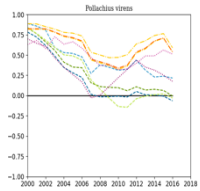	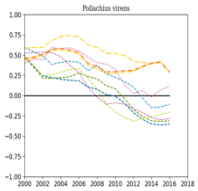	Not enough data	Not enough data
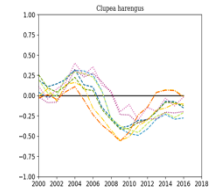	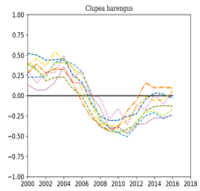	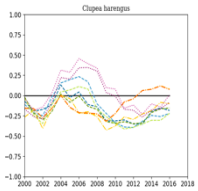	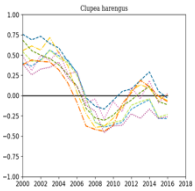	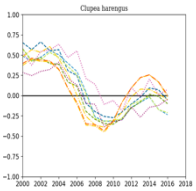
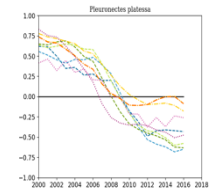	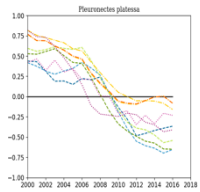	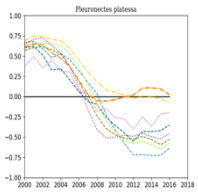	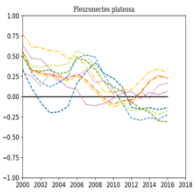	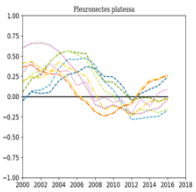

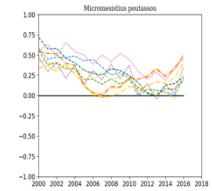	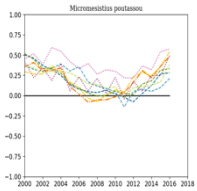	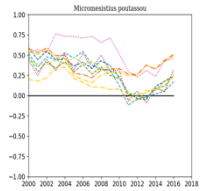	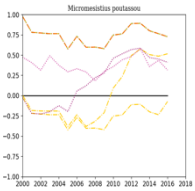	Not enough data
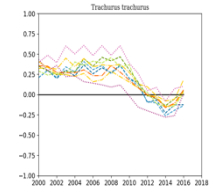	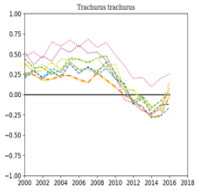	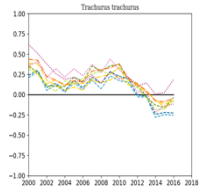	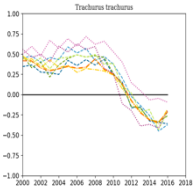	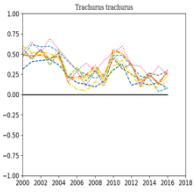
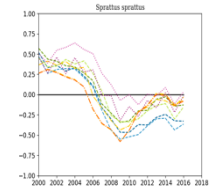		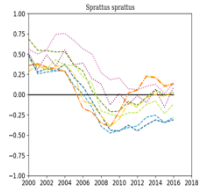	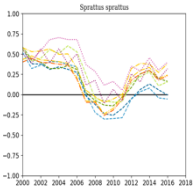	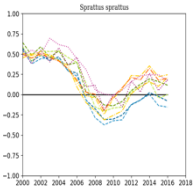
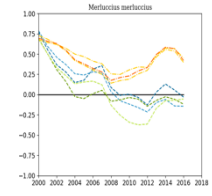	Not enough data	Not enough data	Not enough data	Not enough data
	Not enough data	Not enough data	Not enough data	Not enough data
Salmo salar – Not enough data				
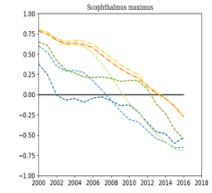	Not enough data	Not enough data	Not enough data	Not enough data
	Not enough data	Not enough data	Not enough data	Not enough data
Hippoglossus hippoglossus – Not enough data				
Mallotus villetus – Not enough data				
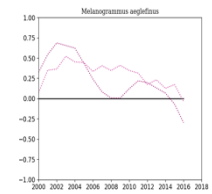	Not enough data	Not enough data	Not enough data	Not enough data

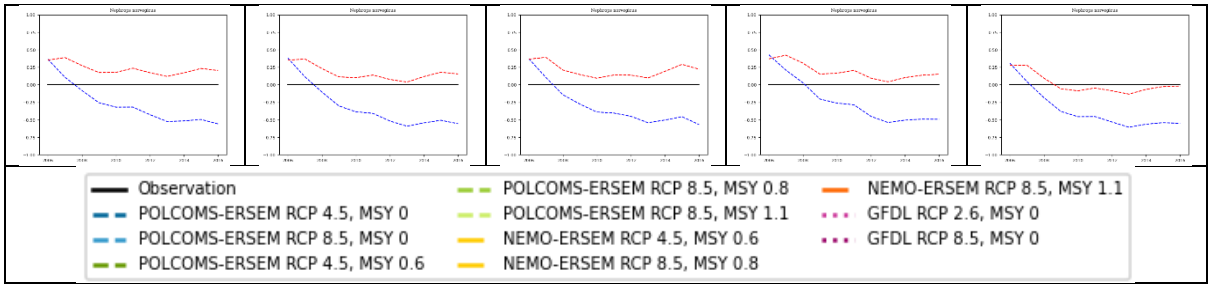

3

5.4.1.3 4Mean difference in temporal trends

This is a different way to look at the difference between model and data (Figures 5.12-5.16). Where the difference might feel overwhelming when looking at it as a trend, when it is reduced to a single value the mismatch is at the 10 year time period instead and reflect the capacity of the model to capture things at a broader time scale rather than on year to year basis. Unsurprisingly, we have a mean that's under 0.5 at the most and in some cases even under 0.25 with it being biased toward an overestimation by the model. It also highlights how for some fish species which model and/or scenario is being used might affect the outcome as we can better see the divergence between the models.

UK EEZ	England	Scotland	Wales	N. Ireland
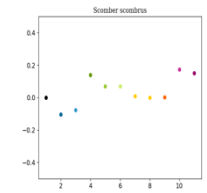	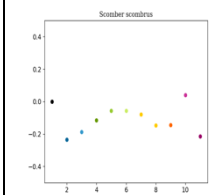	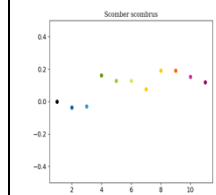	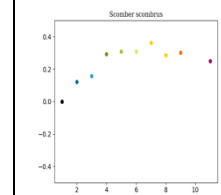	Not enough data
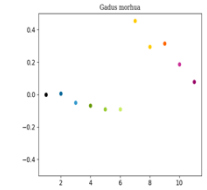	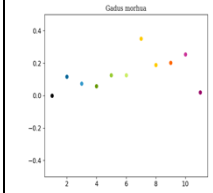	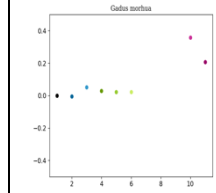	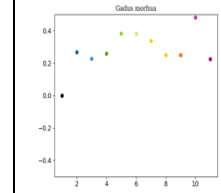	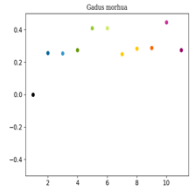
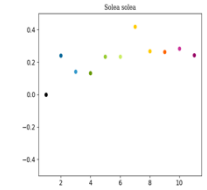	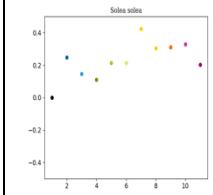	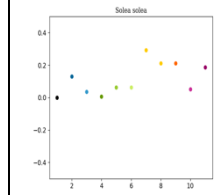	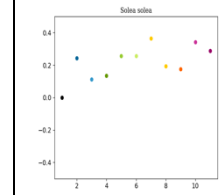	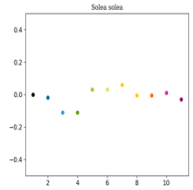
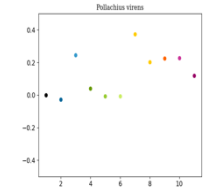	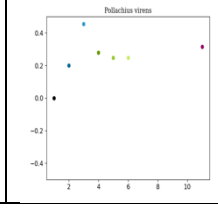	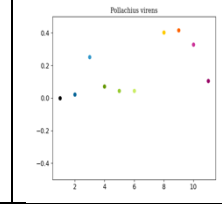	Not enough data	Not enough data

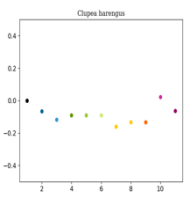	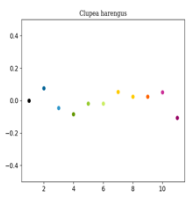	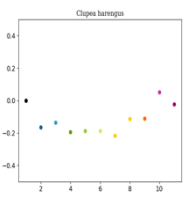	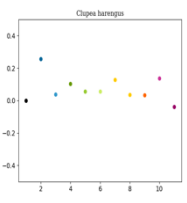	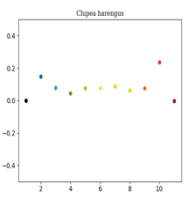
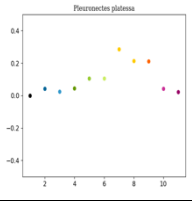	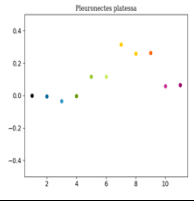	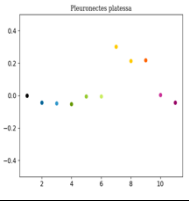	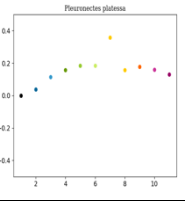	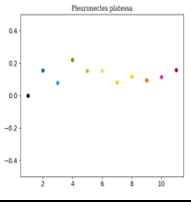
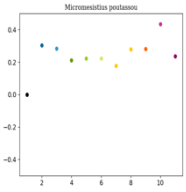	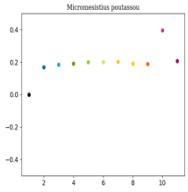	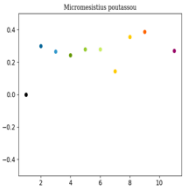	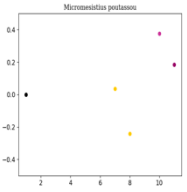	Not enough data
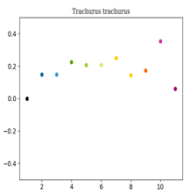	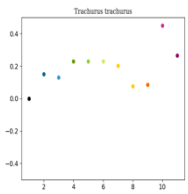	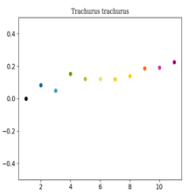	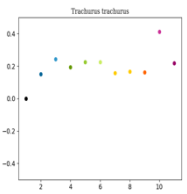	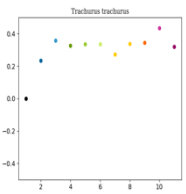
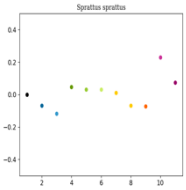	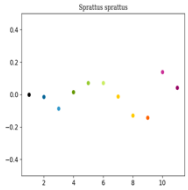	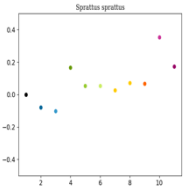	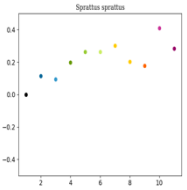	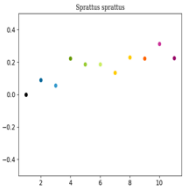
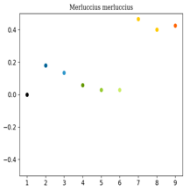	Not enough data	Not enough data	Not enough data	Not enough data
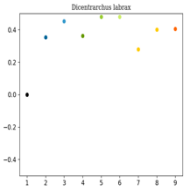	Not enough data	Not enough data	Not enough data	Not enough data
Salmo salar – Not enough data				
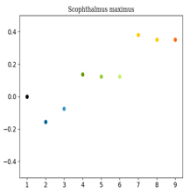	Not enough data	Not enough data	Not enough data	Not enough data

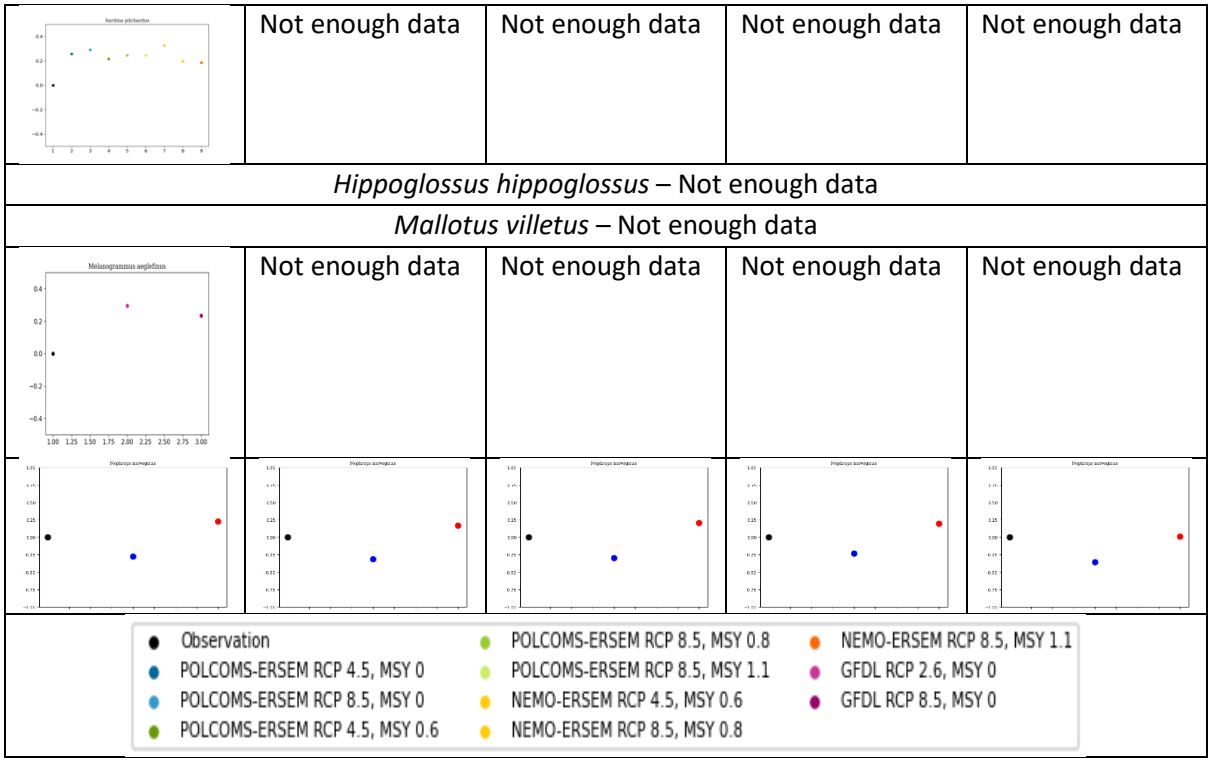

Figure 5.5: Mean difference in the temporal trend between data and model. UK EEZ.

67

5.4.2 Spatial variability

For the spatial variability it was important to match the data points between survey and model outputs to ensure we were comparing a similar geographical spread. As it is at the UK EEZ scale there are areas where there is a lack of data. This is even more critical for the Wales and Northern Ireland National Marine Plan which are smaller than the England and Scotland ones. Plotting all occurrence of sampling against model data (with the model data limited to the UK EEZ) shows that there are some gaps, additionally, not all locations are sampled every year meaning that there are actually much less data on the spatial scale (Figure 5.17, left column for density distribution of survey data).

Consequently, the standard deviation and mean value in the data even when creating a time average of the data is much less than that of the outputs. This is true for all fish and limits the validation that can be done spatially, without presenting a result biased against the model output. As such we need to visually evaluate whether the model and data present some similar patterns for high abundance areas. To this end we mapped the abundance found in the survey and model. While, we limited the model data to the UK EEZ, the full dataset from the survey was used. There isn't a lot of hot spot appearing in the data (Figure 5.17, middle column) compared to the distribution patterns that are visible in the model (Figure 5.17, right column). However, the areas that are most sampled during the surveys (dark red in the maps in the left column) do correspond to the high abundance areas in the model (green to yellow dots). It makes sense that the sampling would happen mostly where the

fish species of interest can be found, indicating that the model captures the distribution of fish species decently well.

Density distribution of survey	Fish distribution - survey	Fish distribution - model
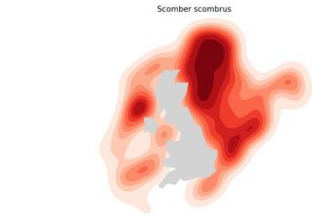	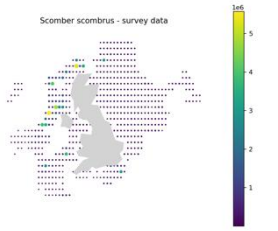	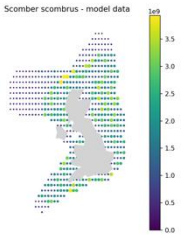
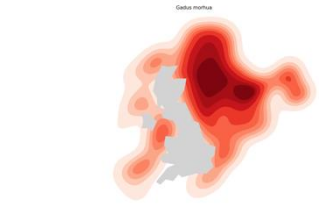	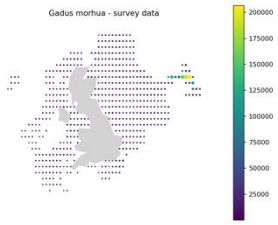	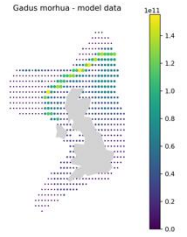
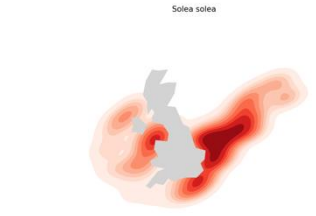		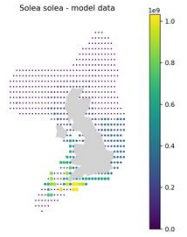
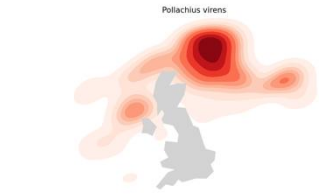	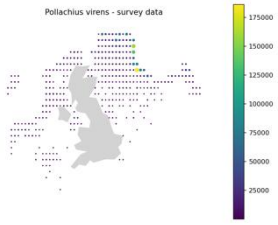	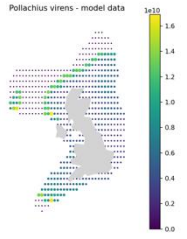
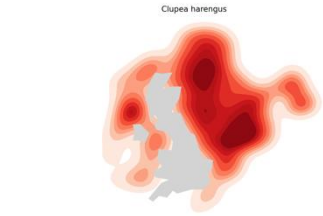	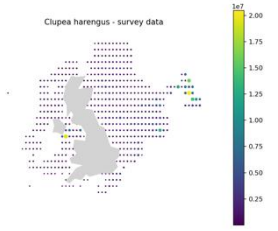	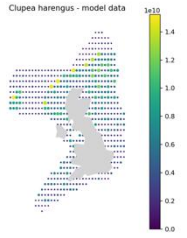

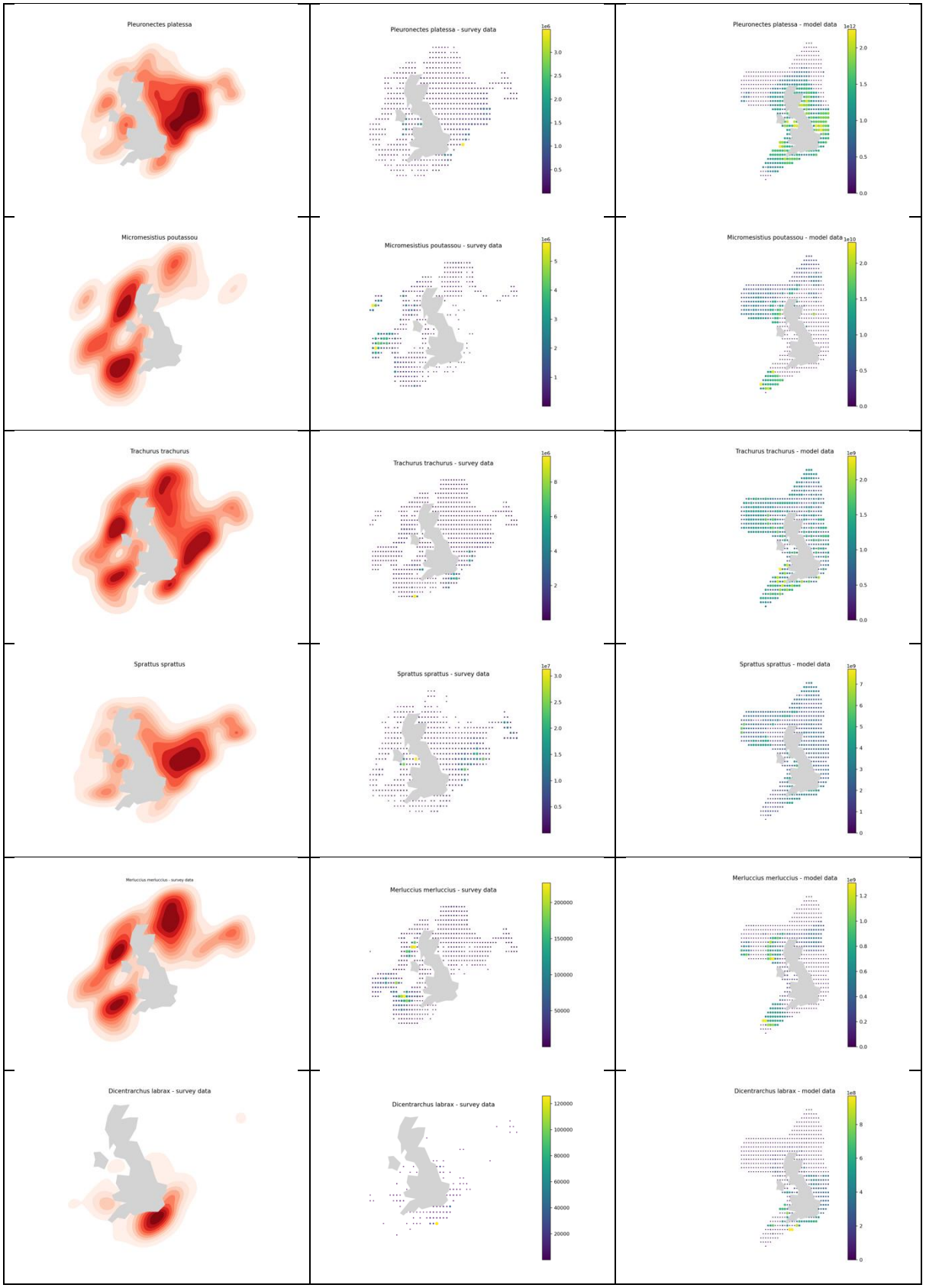
Pleuronectes platessa
Pleuronectes platessa - survey data
Pleuronectes platessa - model data
Micromesistius poutassou
Micromesistius poutassou - survey data
Micromesistius poutassou - model data
Trachurus trachurus
Trachurus trachurus - survey data
Trachurus trachurus - model data
Sprattus sprattus
Sprattus sprattus - survey data
Sprattus sprattus - model data
Merluccius merluccius - survey data
Merluccius merluccius - survey data
Merluccius merluccius - model data
Dicentrarchus labrax - survey data
Dicentrarchus labrax - survey data
Dicentrarchus labrax - model data

Salmo salar Too few data	6 survey site	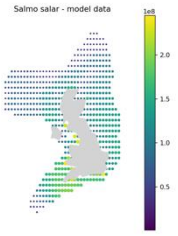
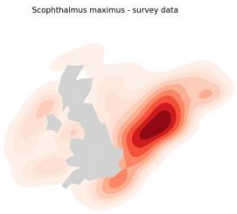	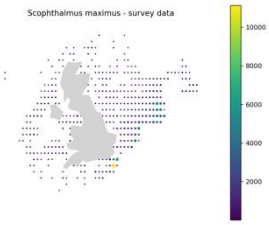	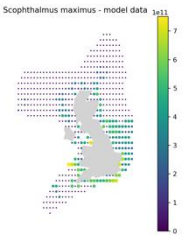
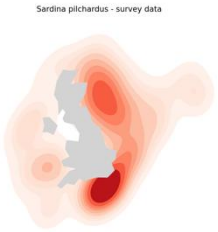	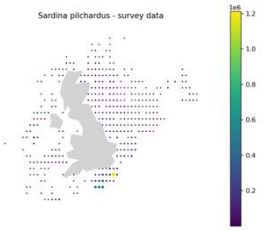	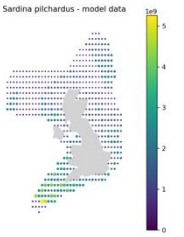
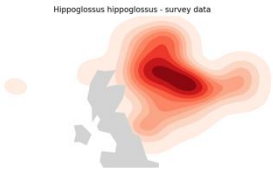	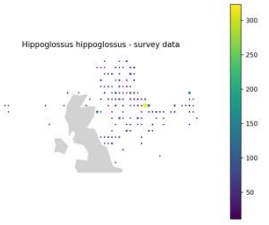	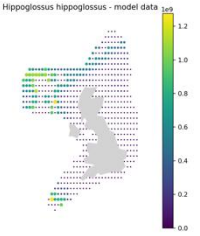
Mallotus villesus No data	No data	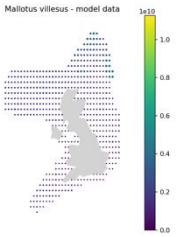
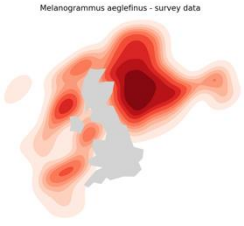	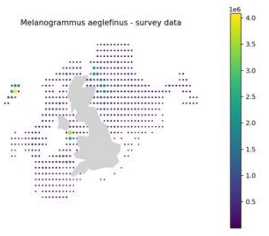	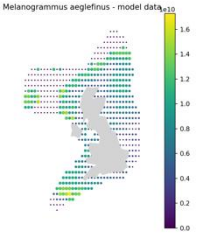

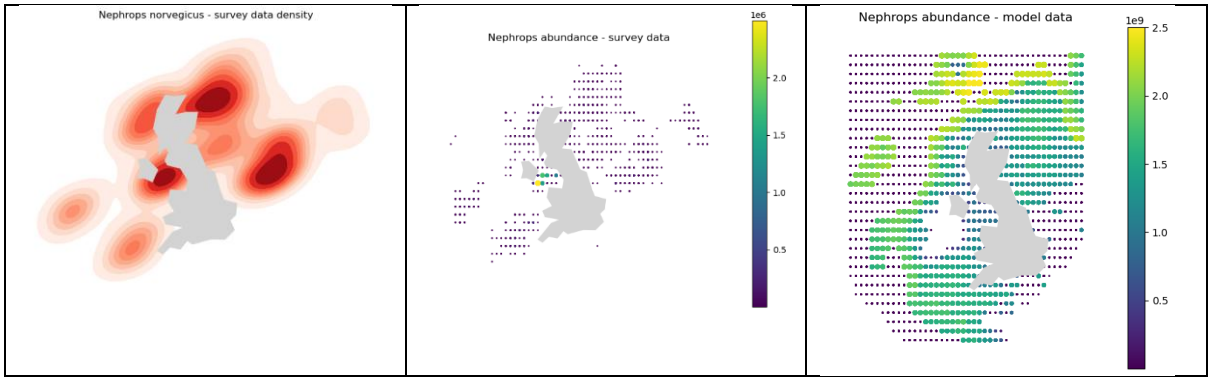

Figure 5.8: Evaluation of the model spatial variation to that found in the data. Left column density distribution of survey data indicating where they are mostly collected. Middle column and right column: sum of abundance of fish per data point expressed as both size and colour of the dots for survey data and model outputs respectively. Survey data are mapped for all data point while the model data are restricted to the UK EEZ.

5.4.3 Short summary

While the capture of the temporal trend was not without fault with an overestimate from the model it was mostly on a year to year basis with the trend over 10+ years being more accurate and reliable. The accuracy of the trend varies between fish species, but overall the model is doing a good job of representing trends in fish. The spatial distribution is more difficult to evaluate because of the sparsity of the data, however there is a match between areas where the model predicts high abundance and those where sampling is most often conducted with the distribution of the data making it to properly see any pattern.

5.5 Expert judgement: confidence in model output

The goal of this section is to provide an evaluation of the model outputs that are used in the meta-analysis for Marine Spatial Planning. While the model cannot provide exact abundance of fish on a year-to-year basis, it is important to see if it can capture trends and variability on the 20 years time scale that we are interested in for long term planning. This focus comes from the fact the meta-analysis is comparing present state against future state. So, while the model might not capture the actual trend and diverge from the survey data on a yearly basis (section 4.1 and 4.2), it might be efficient at capturing the 10 to 20 years signal which are shown through the evaluation of the temporal trend and the spatial distribution.

Additionally, the difference between the model and the observation can be due to bias in either. However, if we consider the bias is consistent (data are corrected for sampling variability in method and location, the model behaviour is consistent and only respond to the change in environmental conditions rather than being erratic and random. As such we're judging model robustness, which can be assessed through the several model scenario that were used in this validation.

The confidence assessment will be caried out for each variable independently, and for each of the areas that were used in this work, this is summarised in Table 5.3 below, fish as well as in the summary of the confidence assessment (section 2).

We are not scoring the model per se but providing an expert judgement on how confident we are in the model, that is whether we are highly confident, confident or less confident. To ensure a coherent judgement on all variables and so users can assess whether they think the scoring is adequate, "scores" are assigned to determine which category the model variable fall into. This is done as follow:

1. Does the model match the data temporal trend or reproduce any pattern that can be found in the data? This is a visual assessment to see if the model at any point match the pattern of the data in the trend plot and is weighted by how many of the models do reproduce the pattern
2. Is the difference between model and data for the temporal trend substantial? This takes into account the difference between model and data trend as well as the mean difference. The more the model deviates from the data (overall and on average) the less confident we are in its capability to capture a long term trend.
3. Is there any spatial match? Is the distribution of fish as presented by the data, matched by the model as well as spots of high density.

Each points is given a "score" from 1 to 3, scores are totalled and divided by 3 for a final score that sits between 1 and 3 to give the final expert judgement as to whether confidence in the model is low, medium or high. In case where there is not enough data we consider this and score it as a "cannot say". The UK EEZ and each notional marine plan area are evaluated separately and the scoring of one fish may be very different between each based on data availability in that region to generate the temporal and spatial metrics (e.g. Pollachius virens data being concentrated in Scotland reflect positively on the scoring for Scotland national marine plan area and the UK EEZ, but not England national marine plan area, and there is not enough data to assess it for the Wales and Northern Ireland national marine plan).

Table 5.3: Expert Judgement scoring of the fish model outputs for each individual fish species. With darker colours indicating higher level of confidence, and grey indicating a lack of data to complete the scoring.

Species of interest	UK EEZ	England	Scotland	Wales	N. Ireland
Clupea harengus					
Dicentrarchus labrax					
Gadus morhua					
Hippoglossus hippoglossus					
Mallotus villeus					
Melanogrammus aeglefinus					
Merluccius merluccius					
Micromesistius poutassou					
Nephrops Norvegicus					
Pleuronectus platessa					
Pollachius virens					
Salmo salar					

Sardina pilchardus					
Scomber scombrus					
Scophtalmus maximus					
Solea solea					
Sprattus sprattus					
Trachurus trachurus					

5.6 References for section 5

Fernandes, J.A., Cheung, W.W., Jennings, S., Butenschön, M., de Mora, L., Frölicher, T.L., Barange, M. and Grant, A., 2013. Modelling the effects of climate change on the distribution and production of marine fishes: accounting for trophic interactions in a dynamic bioclimate envelope model. Global change biology, 19(8), pp.2596-2607. https://doi.org/10.1111/gcb.12231

Cheung W.W.L., Close C., Kearney K., Lam V., Sarmiento J., Watson R., Pauly D., 2009. Projections of global marine biodiversity impacts under climate change scenarios. Fish and Fisheries, 10, 235–251. https://doi.org/10.1111/j.1467-2979.2008.00315.x

Fernandes, J. A., Rutterford, L., Simpson, S. D., Butenschön, M., Frölicher, T. L., Yool, A., … Grant, A. (2020). Can we project changes in fish abundance and distribution in response to climate? Global Change Biology, 26(7), 3891–3905. https://doi.org/10.1111/gcb.15081

6 Brown crab *(Cancer pagarus)*; DEB model

6.1 Model description

DEB model parameters for *Cancer pagurus* were taken from the Add-my-Pet database (Kooijman, 2017), which contains DEB parameters for >1000 species. The goodness of fit between observed data and DEB model predictions is quantified using mean relative error (MRE) and symmetric mean squared error (SMSE), with values closer to zero indicating a better match between data and predictions. MRE is 0.098 and SMSE is 0.02 for predictions made using these parameters (Kooijman, 2017). The temperature dependence of physiological rates is accounted for in the DEB model by the Arrhenius temperature, which is calculated from the observed values of physiological rates such as metabolic or growth rate at various temperatures. There was no specific evaluation of the robustness of this Arrhenius temperature provided with the parameter set used in this model. Full details of the parameters used, and the data used to validate predictions, are available from the Add-my-Pet species list.

The DEB model used in these analyses was forced using POLCOMS-ERSEM projections for bottom layer temperature and depth integrated NPP (as a proxy for food availability), initially generated for the CERES project (Kay, 2018). The model made predictions for three physiological endpoints – ultimate size MC (measured as carbon mass, g), age-at-maturity AAM (days) and cumulative

allocation to reproduction over the whole of the modelled time period M_R (gC). As any increase in temperature will lead to an increase in metabolic rates, it was assumed that M_R (allocation to reproduction integrated over a fixed time period) would likely increase in the future due to predicted ocean warming. However, increased metabolism will also lead to increased natural (and possibly predation) mortality, which may negate any temperature driven gains in M_R. While survival is not explicitly modelled, future estimates of M_R were temperature corrected to try and account for this. DEB models use a temperature correction factor (TC) to describe the temperature dependency of physiological rates. For each POLCOMS-ERSEM model grid cell a "metabolic speedup factor" was calculated ($TC_{future}/TC_{present}$). Future predictions of M_R were divided by this factor. The model does not directly predict *C. pagurus* presence/absence or population dynamics – it evaluates an individual's potential to grow and allocate energy to maturation and reproduction over the whole model domain. However, population level inferences can be made using the reproductive endpoints AAM and M_R. The possible distribution of *C. pagurus* populations in each time period was estimated by allocating the values of each of these endpoints in each model grid cell a "viability score". These scores were based on the notion that individual fitness is determined by the amount of carbon an individual invests in reproduction over its lifetime. Areas in which animals mature early and are able to invest heavily in reproduction therefore produce individuals with the greatest fitness, and so have the highest viability scores. Individual scores were summed and normalised to give an overall viability score for each grid cell between 0 and 1, with 0 indicating that the area would be unlikely to support a population, and 1 indicating an area would be very likely to support a population.

6.2 Validation methodology

A formal evaluation of the distributions predicted by the *C. pagurus* model used in this analysis was not conducted. The model outputs were assessed by visual comparison of the viability scores (Figure 6.1a) to the probability of occurrence data projected by Aquamaps (Figure 6.1b) and recorded occurrence data provided by NBN Atlas (Figure 6.1c).

6.3 Validation outcomes

The spatial patterns of distribution projected by the DEB model are broadly correct around most of the UK. The only exception appears to be in the deeper parts of the Western English Channel where the DEB model projects high viability scores (Figure 6.1a). This is not in keeping with the projected probability of occurrence (Figure 6.1b) or the recorded occurrence data (Figure 6.1c) for this area. Despite this however, we can be confident in the spatial component of the DEB outputs used in the spatial meta-analysis because of the good agreement elsewhere.

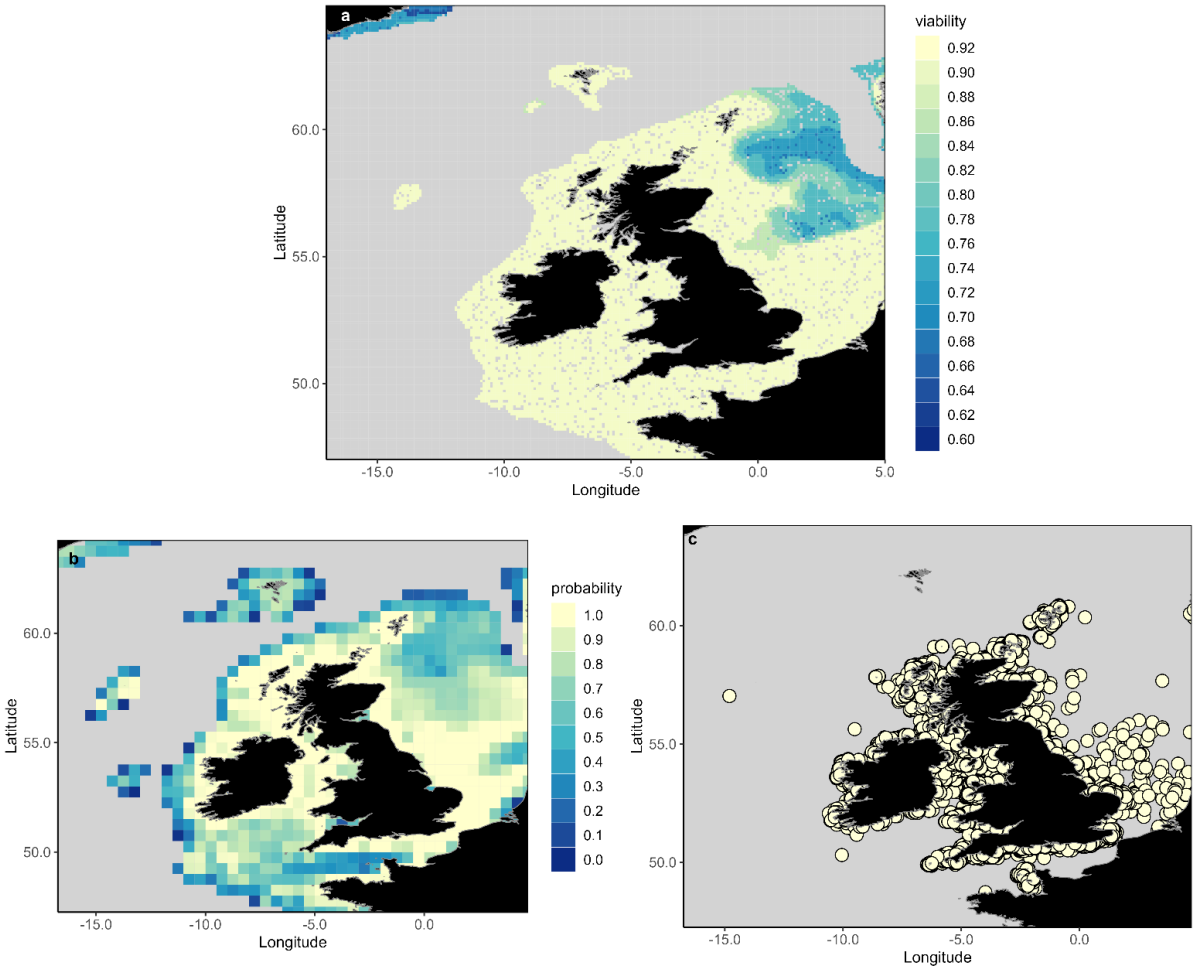

Fig. 6.1: a) Projected present day (2022) distribution of *Cancer pagurus* based on viability scores derived from DEB model endpoints; b) projected present day probability of occurrence of *Cancer pagurus*, downloaded from Aquamaps; c) confirmed occurrences of *Cancer pagurus* between 1948 and 2022, downloaded from the National Biodiversity Atlas.

In order to establish whether the temporal trend in distributions was robust, DEB model projections for 2050 (Figure 6.2a) under RCP8.5 were visually compared to the RCP8.5 2050 native range map generated by Aquamaps (Figure 6.2b). DEB model projections show a small decrease in viability scores across most of the UK EEZ, with the exception of the northern North Sea, where scores increase slightly in comparison to present day projections. These apparent changes in habitat suitability do not appear to be replicated in the Aquamaps projections for 2050, however the spatial patterns of distribution are comparable between the two model outputs, despite the small differences. Therefore, we can be moderately confident that the trend of the projections from the DEB model are robust.

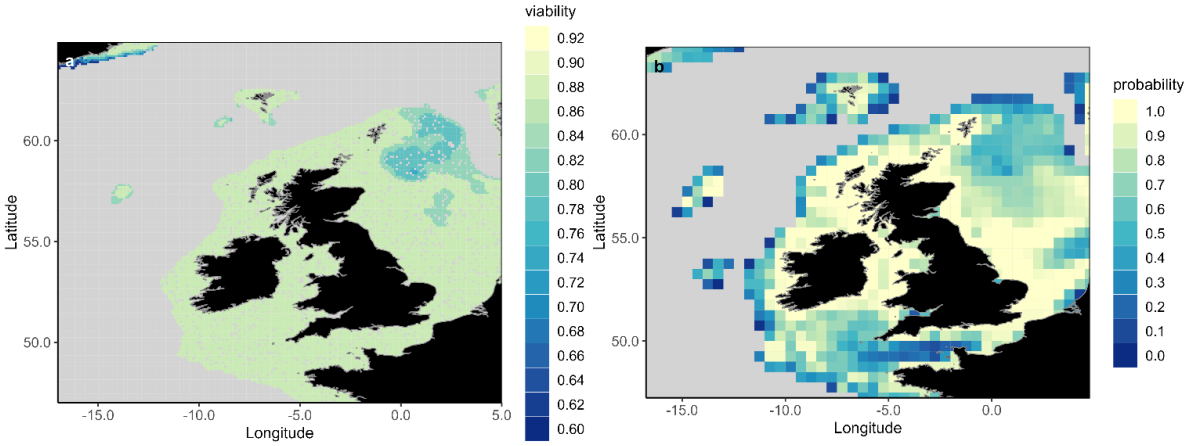

Fig. 6.2: a) Projected future (2050) distribution of *Cancer pagurus* based on viability scores derived from DEB model endpoints; b) projected 2050 probability of occurrence of *Cancer pagurus*, downloaded from Aquamaps

6.4 References for section 6

Add my Pet (AmP) species list:
https://www.bio.vu.nl/thb/deb/deblab/add_my_pet/entries_web/Cancer_pagurus/Cancer_pagurus_res.html

AquaMaps, Nov. 2022. Computer generated distribution maps for *Cancer pagurus* (edible crab), with modelled year 2050 native range map based on IPCC RCP8.5 emissions scenario. Retrieved from https://www.aquamaps.org.

Kooijman, 2017. AmP *Cancer pagurus*, version 2017/08/25.

National Biodiversity Atlas (NBN) Atlas *Cancer pagurus* occurrence download at https://spatial.nbnatlas.org/?fq=(lsid:NBNSYS0000174336%20AND%20occurrence_status:present). Accessed 21 November 2022.

7 Seaweed (sugar kelp, *Saccharina latissima*); DEB model by Broch et al., 2012

7.1 Model description

Future *S. latissima* (sugar kelp) aquaculture production was projected using the Dynamic Energy Budget (DEB) model from Broch et al. (2012). The DEB uses temperature, nitrate concentration and photosynthetically active radiation to represent the seasonal growth of kelp frond. Aquaculture production was simulated following the approach of Broch et al. (2019). Using their initial "seed" conditions, we grew kelp from September to June in each annual season from 2000-2099. For each season we recorded the maximum size of the kelp to estimate how annual production could be impacted by climate change. Driving conditions were taken from ERSEM projections for RCP 4.5 and 8.5. Photosynthetically Active Radiation (PAR) reaching kelp was estimated using sea-surface PAR

and light attenuation (KD490) from version 4.3 of the Ocean Colour Climate Change Initiative (https://www.oceancolour.org/) product.

7.2 Validation methodology

Confidence was assessed on the basis of previously published validation of the model.

7.3 Validation outcomes

The model has previously been validated at regional scales in Broch et al. (2012, 2019) and Jiang et al. (2022). The DEB model has been shown to be able to reproduce the seasonal cycle of sugar kelp growth (Broch et al. 2012, Jian et al. 2022). At present due to the lack of long-term data no studies have evaluated whether the model is ability to reproduce inter-annual variation in sugar kelp growth. However, the optimum temperatures for growth and photosynthesis are reasonably well constrained (Bolton and Luning 1982). We therefore have moderate to high confidence in the response of kelp to changing temperatures. Given the strong confidence in the POLCOMS-ERSEM surface temperature and moderate to weak confidence in the bottom-level temperature, we assess confidence in the seaweed dataset as moderate overall.

7.4 References for section 7

Bolton, J. J., & Lüning, K. (1982). Optimal growth and maximal survival temperatures of Atlantic Laminaria species (Phaeophyta) in culture. *Marine Biology*, *66*(1), 89–94. https://doi.org/10.1007/BF00397259

Broch, O. J., & Slagstad, D. (2012). Modelling seasonal growth and composition of the kelp Saccharina latissima. *Journal of Applied Phycology*, *24*(4), 759–776. https://doi.org/10.1007/s10811-011-9695-y

Broch, O. J., Alver, M. O., Bekkby, T., Gundersen, H., Forbord, S., Handå, A., Skjermo, J., & Hancke, K. (2019). The kelp cultivation potential in coastal and offshore regions of Norway. *Frontiers in Marine Science*, *5*(JAN), 1–15. https://doi.org/10.3389/fmars.2018.00529

Davison, I. (1986). *Adaptation to photosynthesis in Laminaria saccharina (Phaophyta) to changes in growth temperature*. *December*.

Jiang, L., Blommaert, L., Jansen, H. M., Broch, O. J., Timmermans, K. R., & Soetaert, K. (2022). Carrying capacity of Saccharina latissima cultivation in a Dutch coastal bay: a modelling assessment. *ICES Journal of Marine Science*, *79*(3), 709–721. https://doi.org/10.1093/icesjms/fsac023